Updates on Beam Dynamics Studies and Emission Modelling at PITZ

Ye Chen, M. Krasilnikov, Darmstadt, June 8th 2018

Contents:

- Introduction
- Follow-ups of coupler kick study
  - ✓ Clarification of traveling-wave effect
  - ✓ Estimation on local emittance growth
  - ✓ Laser beam based alignment
- Photoemission modeling: status and new approach
- On dark current issue
- Summary

Gun4.5 installation into the PITZ beamline and baking of the gun system

PITZ evolution 2000-2017

	Year-->	2002	2003	2004	2005	2006	2007	2008	2009	2010	2011	2012	2013	2014	2015	2016	2017
gun	cavity	gun-2	FLASH	gun-1		gun-3.1 FLASH	g-3.2	gun-4.2	FLASH	gun-4.1		FLASH g-3.1	4.3 XFEL	g-4.4 XFEL*	gun-4.2	gun-4.6	XFEL g-4.5
gun	Ez,MV/m	35	37	42-->60		43	60										
gun	Ebeam	~4MeV		4.3MeV-->6MeV		4.5MeV	~6.5MeV										
boo	cavity	no			TESLA at 2.5m		TESLA at 3.1m			CDS at 3m				CDS at 2.6m			
boo	Ebeam				~13MeV					~25MeV			22MeV*				
laser	temp ps	10	6/24\6	-->			6/24\6	2/22\2	-->					2/22\2	11*		
emit	EMSY1	z=1.618m			z=4.3m		z=5.74m							z=5.277m			
emit	Ldrift	1.01m			2.334m		2.64m							3.133m			
emit	method	center BL	3xBLs		e-meter	11xBLs			detailed scan							+slice with TDS	
emit	min ε_{xy} mm mrad (charge)		3 (1nC)	1.5-1.7 (1nC)		1.37 (1nC)	1.26 (1nC)		0.9 (1nC)		0.7 (1nC)				0.8 (0.5nC)		
PITZ goals		small emittance (nominal EXFEL)										+reliability at full performance			+emittance (EXFEL startup)		
												+THz		+plasma			

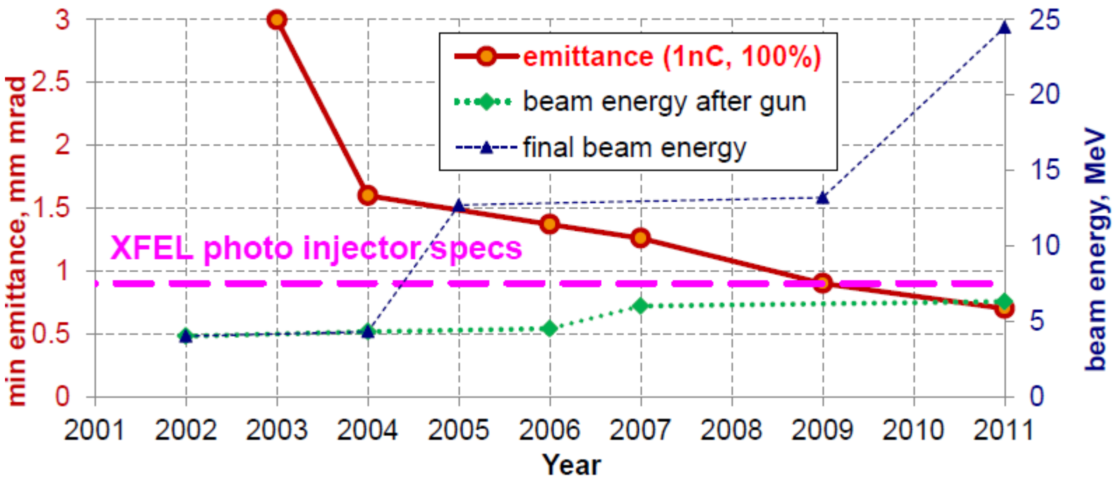

Highlights of the Evolution:

→Increasing the brightness (decreasing the emittance)

→Improving gun stability and reliability

→Extending beam diagnostics

→Use high brightness beam capability

Improving beam quality

Experimental compensation for beam asymmetries

On RF coupler:	Proc. FEL 2017, WEP005
On gun quads:	Proc. FEL 2017, WEP007
On quadrupole field error:	Proc. FEL 2017, WEP010

- **Demonstration for a 500 pC bunch of 22 MeV/c**

Guan quadrupoles off

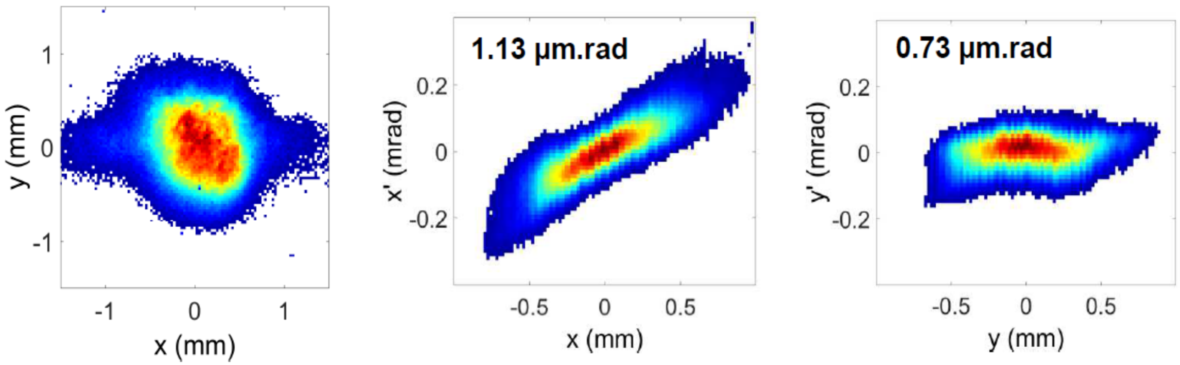

Guan quadrupoles on

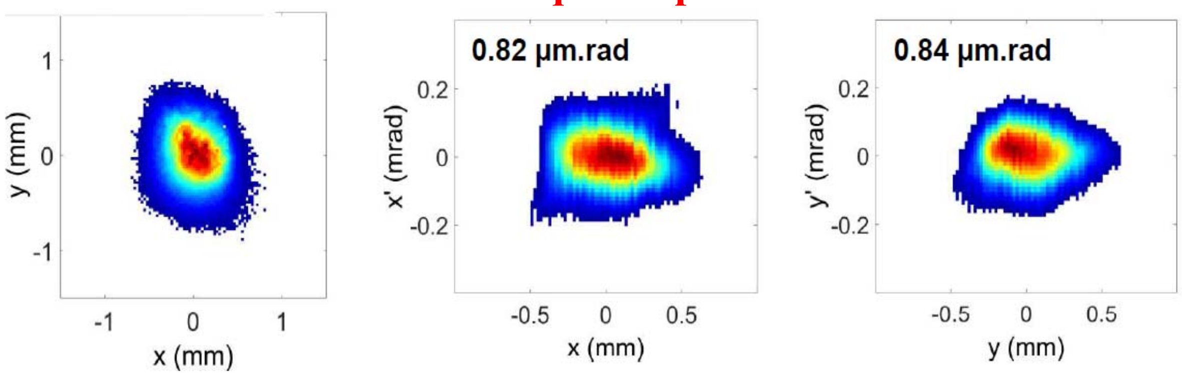

- Gun quads compensate rotational **asymmetry of gun RF field and solenoid field**, improve both beam symmetry and emittance.
- Three copies are installed at **PITZ, XFEL, FLASH**

Improving beam quality

Explain remaining discrepancies in beam dynamics simulation w.r.t. experiment

ASTRA simulations
for **Gaussian pulses** (2017) using Core + Halo

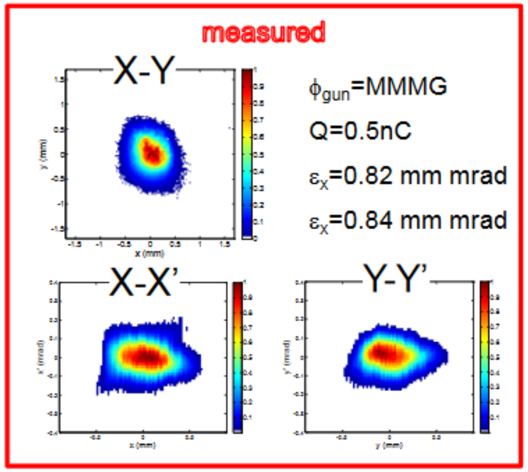

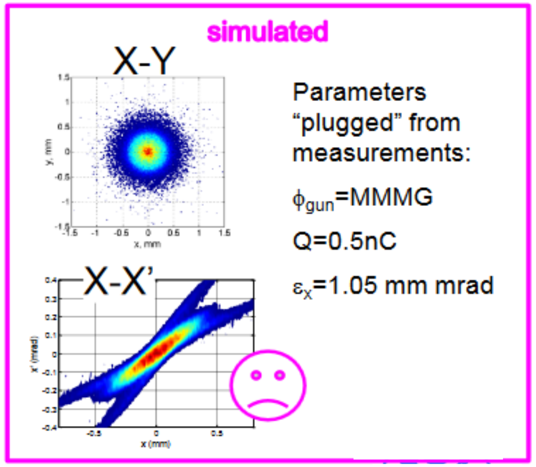

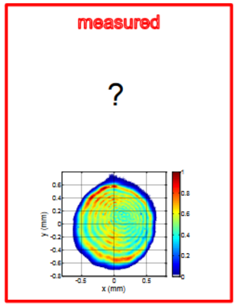

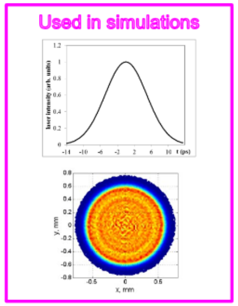

ASTRA simulations
for **flattop pulses (2011)** using Core + Halo

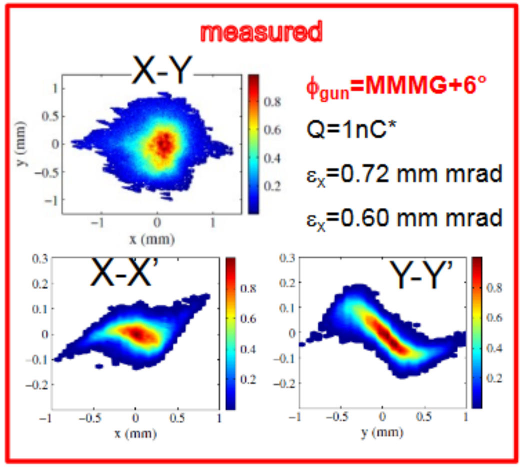

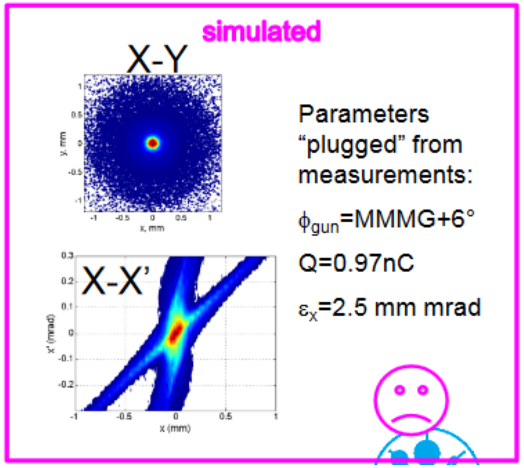

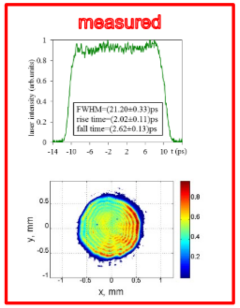

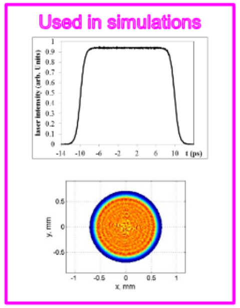

Improving beam quality

Explain remaining discrepancies in beam dynamics simulation w.r.t. experiment

ASTRA simulations
for **Gaussian pulses** (2017) using Core + Halo

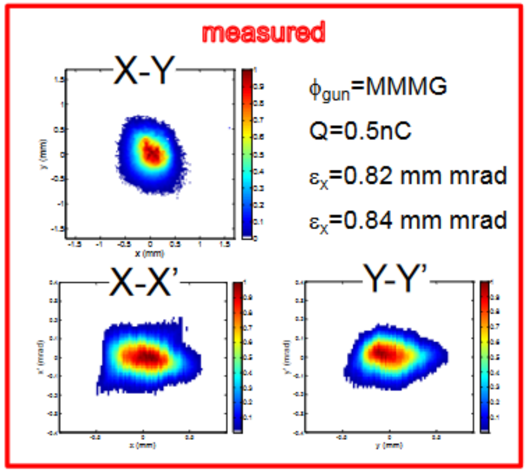

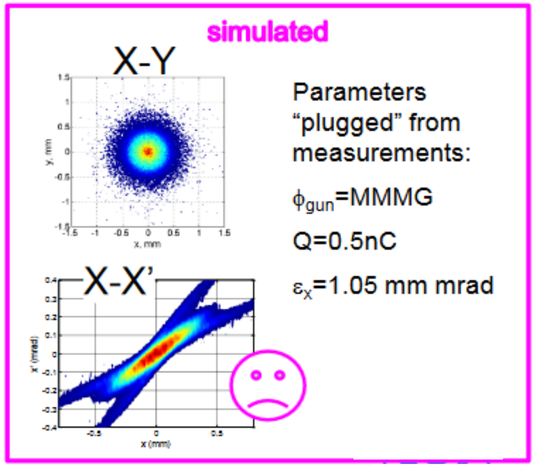

ASTRA simulations
for **flattop pulses (2011)** using Core + Halo

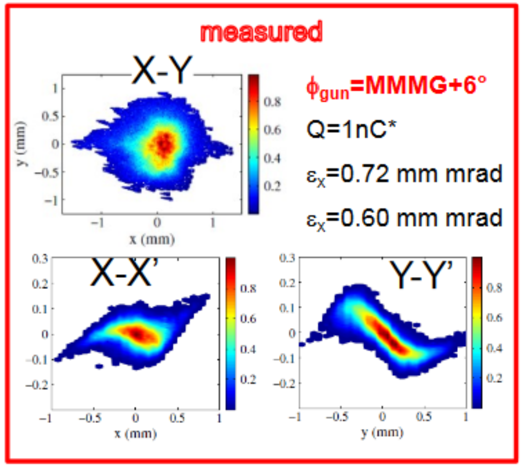

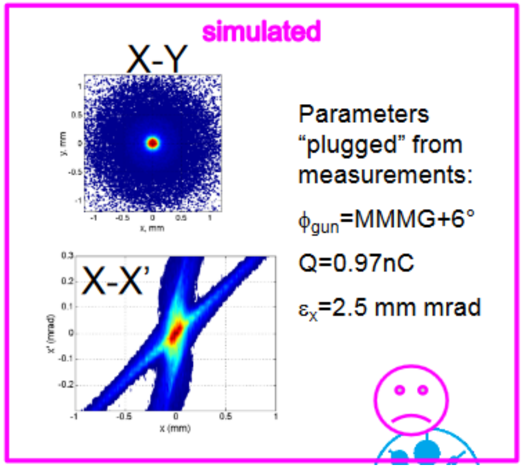

To improve beam dynamics simulations

→ emission modeling
→ coupler kick simulations
→ solenoid field simulations
→ simulations with rotational quads model for fitting measurements
→ gun quadrupole designs and simulations
→ gun quads compensation for emittance
→ etc.

Impacts of "traveling-wave effect" on beam dynamics
— Motivation

1. **Dipole kick** resulted from door-knob transition can be **eliminated by** using **symmetrical coupler**
2. **Not clear:** effect(s) due to the ***traveling wave*** by the end of the coaxial line on beam dynamics

Sketch of PITZ gun

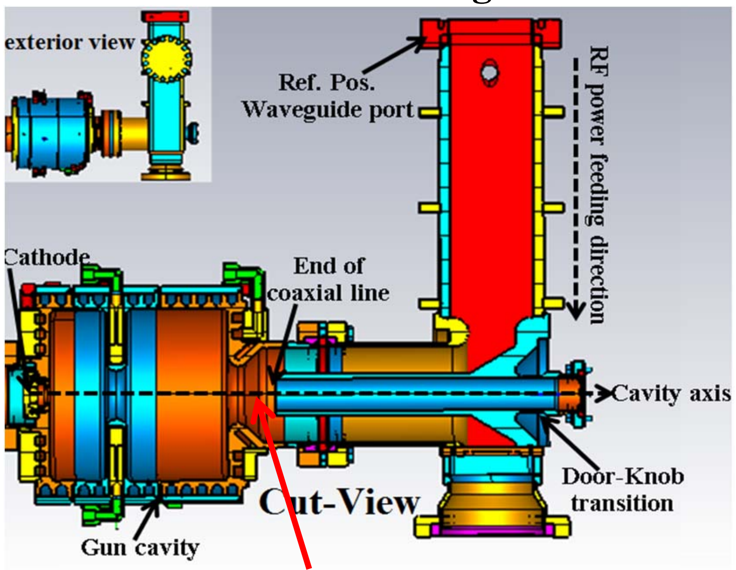

3. **If** some effects, they **may still be present** even with a symmetrical coupler design
4. **If** some effects, instead of a given **Ez profile** (paraxial) calculated from the **Eigenmode,** necessary to use **a (traveling) field map** for regular Astra simulations?

Computational model and field calculation

Gun Model

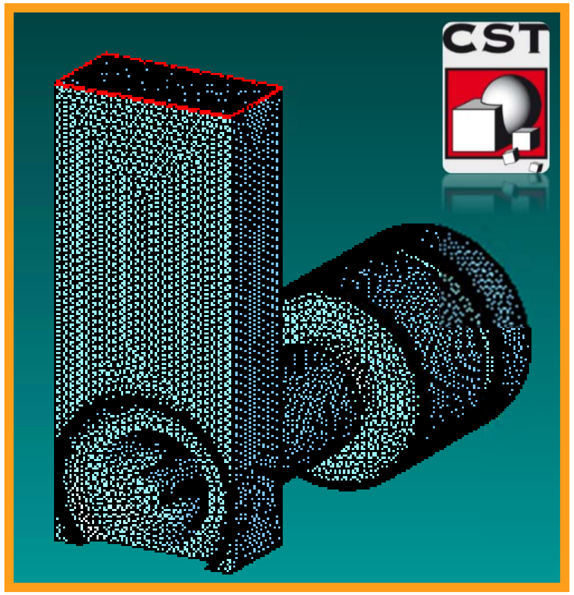

- → **Frequency domain (F-) solver**
  - → mono-frequency excitation
  - → broadband matching from WG to coaxial line
  - → narrowband matching from coaxial line to cavity
- → **Meshing affecting field accuracy, important for kick calculation**

RF field components on cavity axis: refining mesh resolution

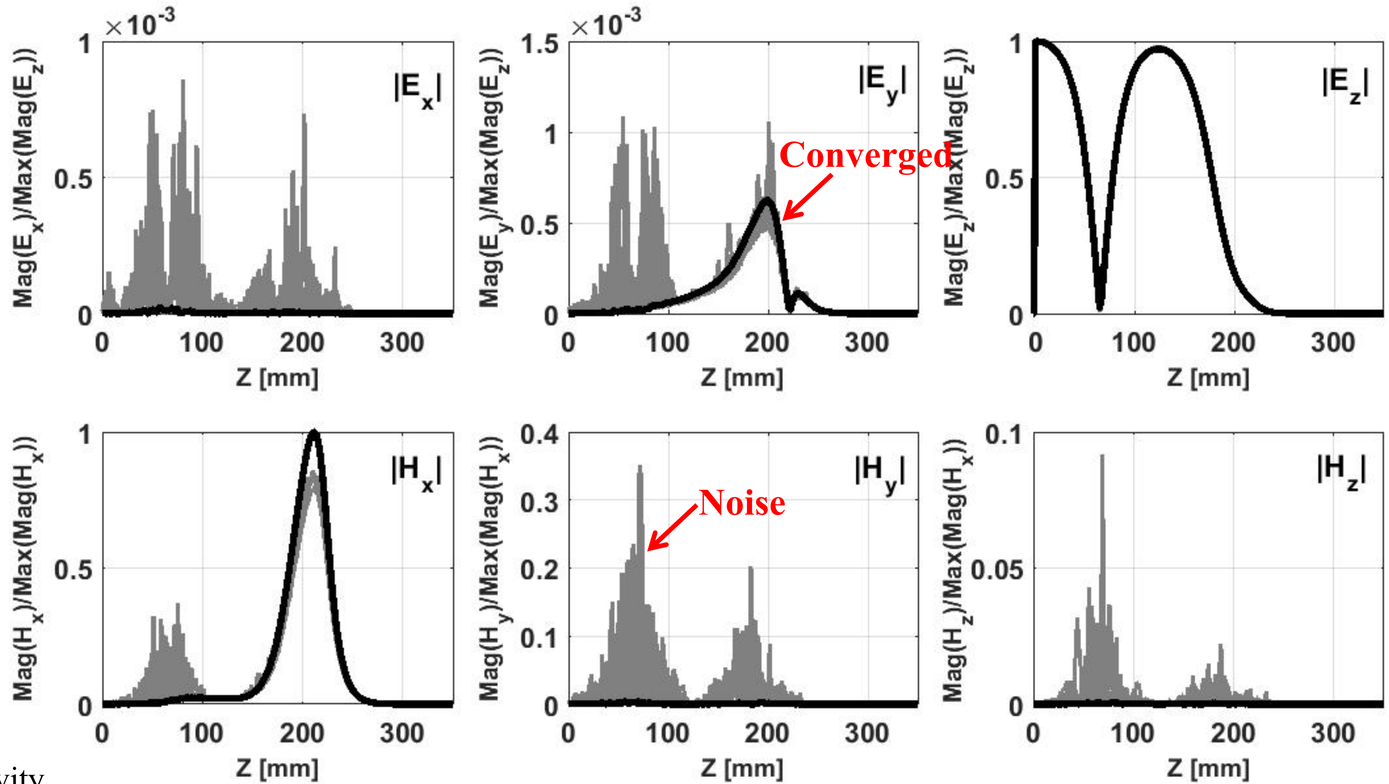

- → A 3D RF field map made based on F-solver calculation **(case abbrev. "traveling")**
- → For comparison of beam dynamics, another field map made based on E-solver calculation **(case abbrev. "standing")**

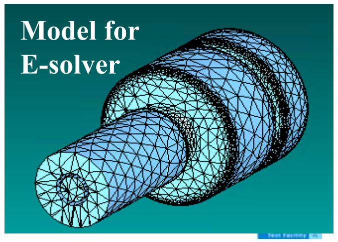

Comparison of Ez profiles, amplitude

Traveling vs. standing

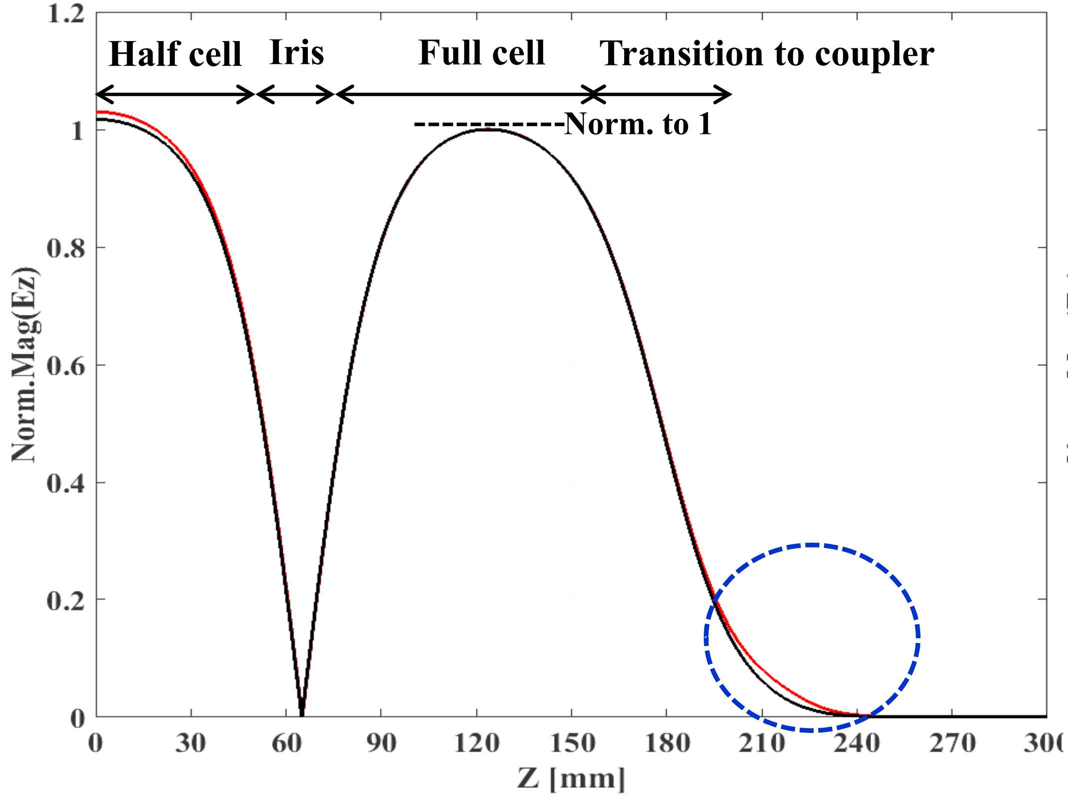

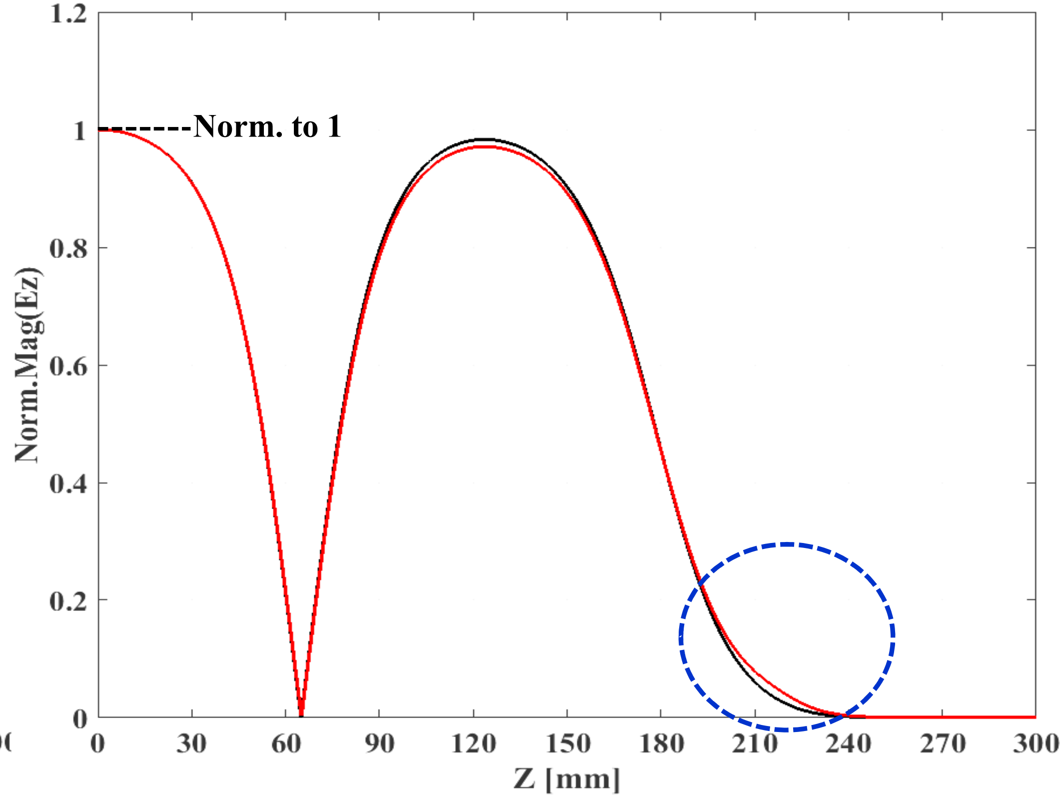

1. Field balance slightly different
2. Field profile differs in the transition region

60.58MV/m (traveling wave) vs. 59.57MV/m (standing wave) for the same momentum, 6.82 MeV/c

Comparison of Ez profiles, phase

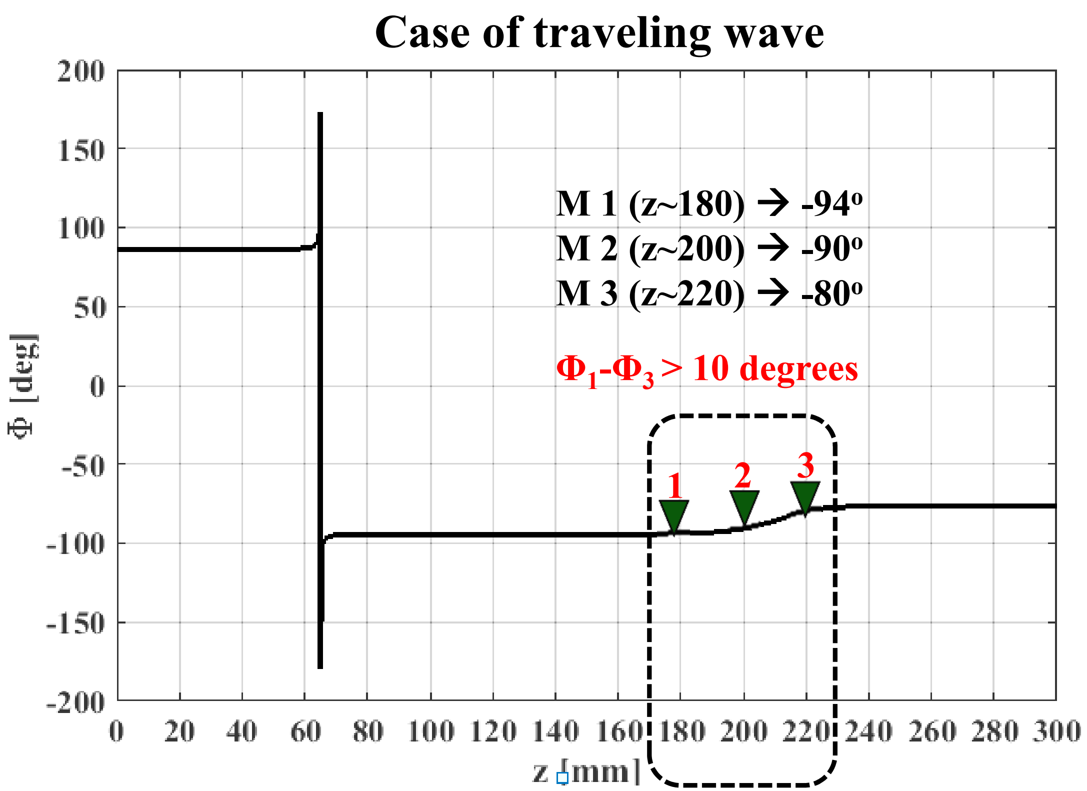

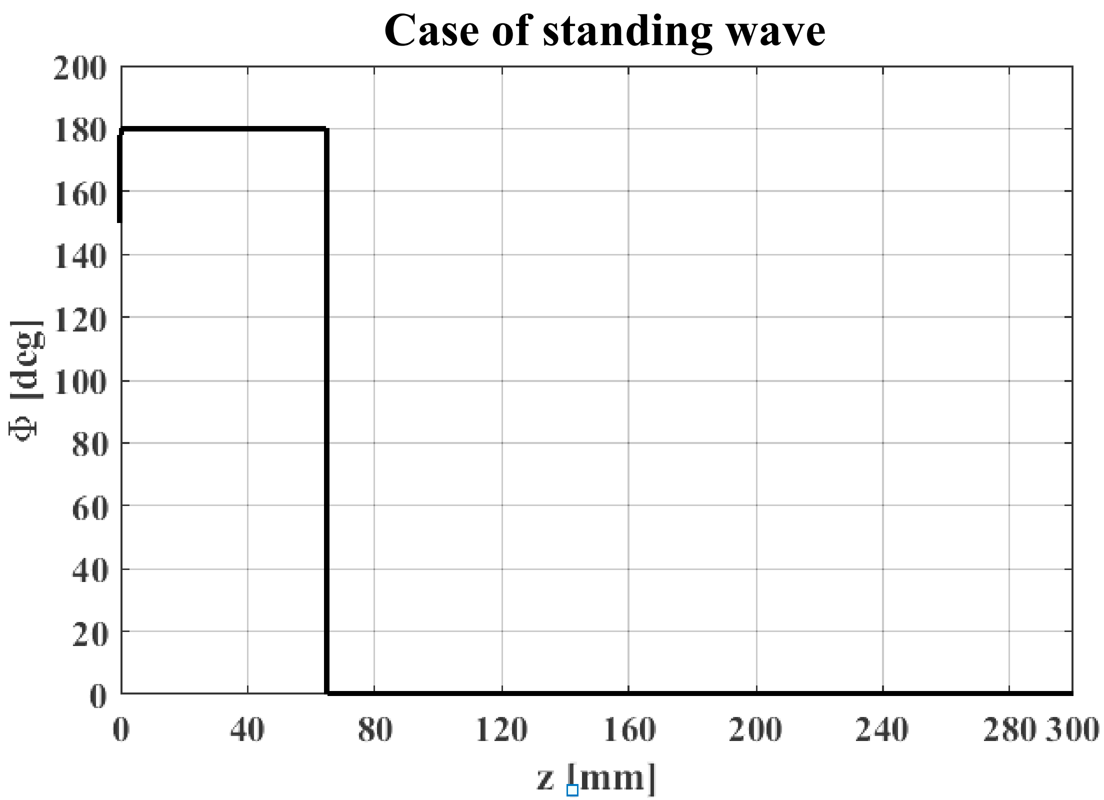

Ez field profile for the case of traveling wave

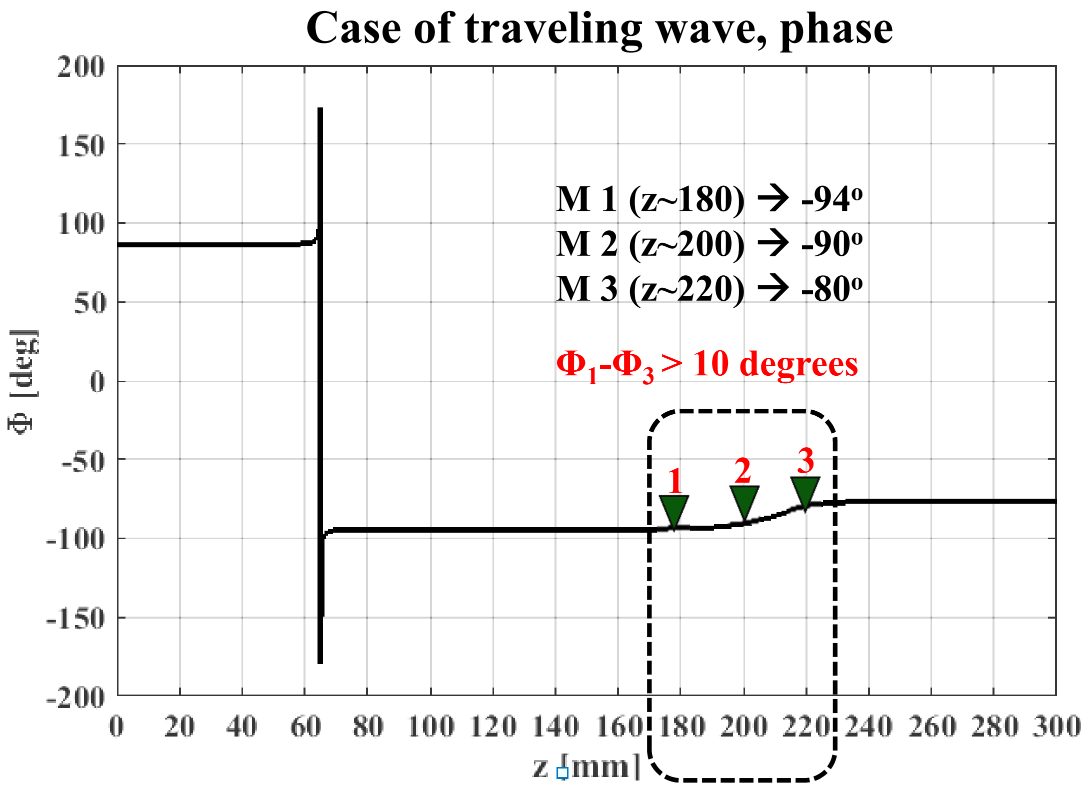

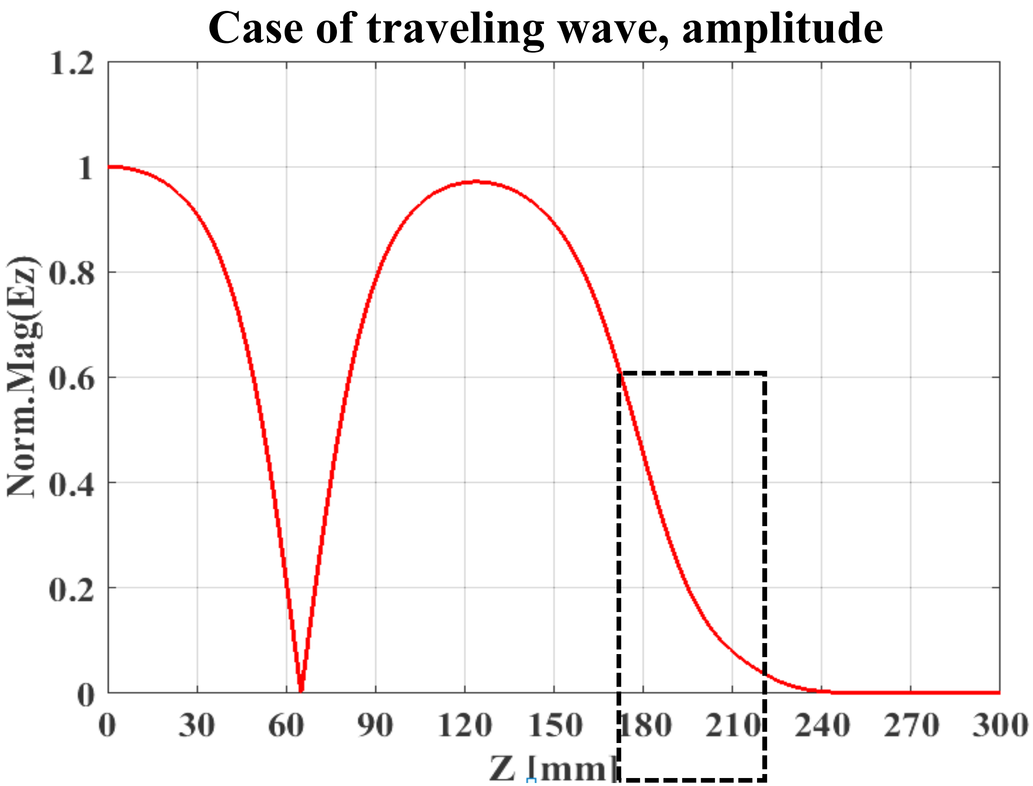

Comparison of beam size at the 1st screen after gun (z=0.8m)

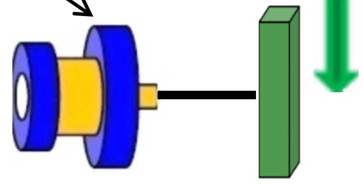

Solenoids OFF, around RF focusing phase

Comparisons of beam sizes at 3 gun phases around the best focusing phase (e.g., laser BBA phases)

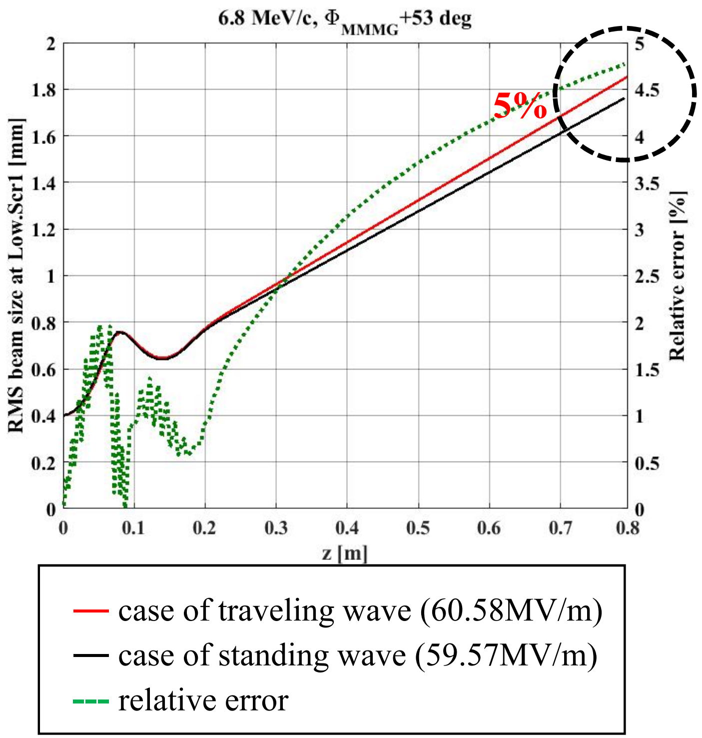

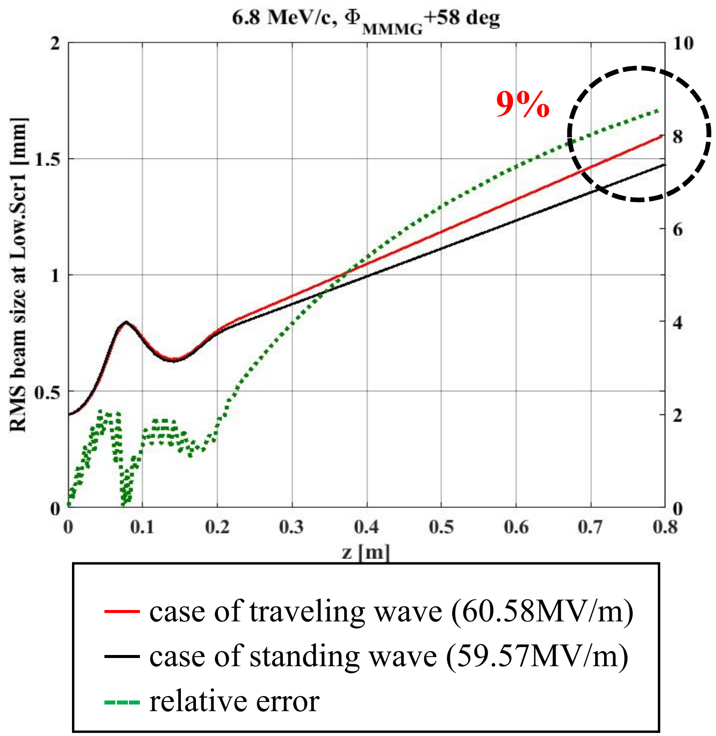

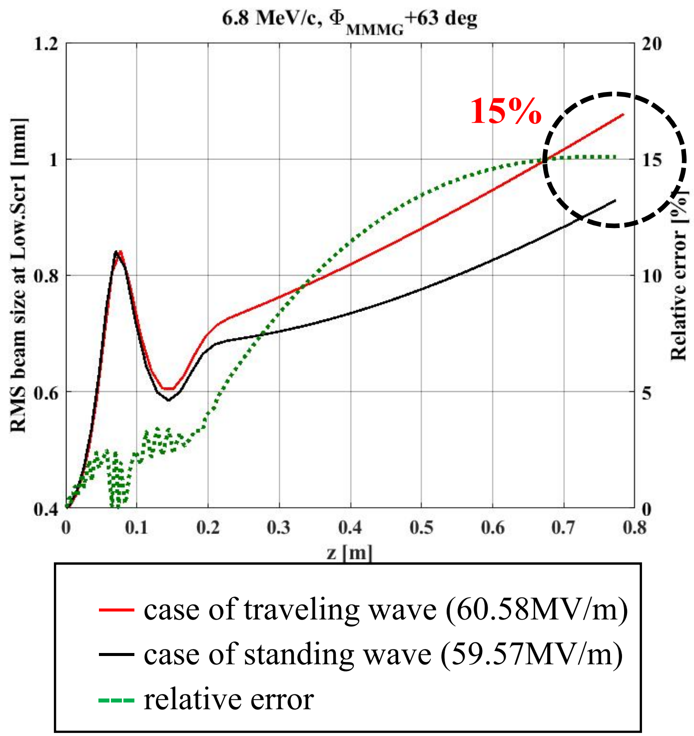

The discrepancies are phase dependent.

ASTRA

Comparison of beam size at the 1st screen after gun (z=0.8m)

Solenoids OFF, around MMMG phase

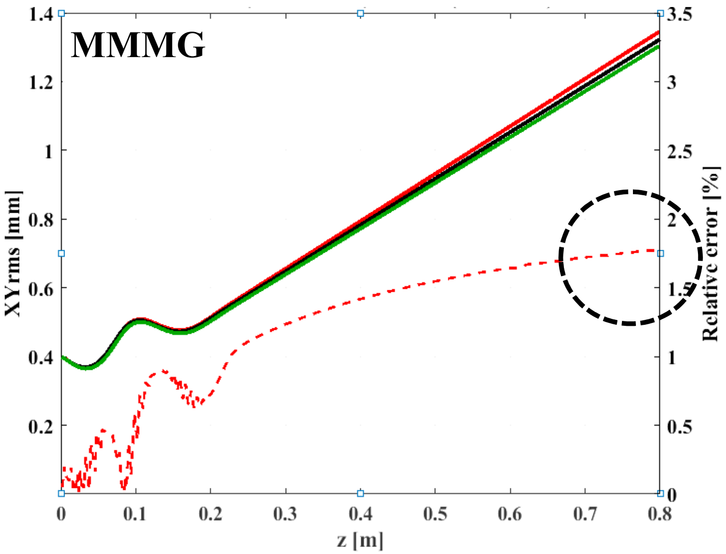

- case of traveling wave (60.58MV/m), **MMMG**
- case of standing wave (59.57MV/m), MMMG
- case of traveling wave, -2 deg off-crest
- relative error

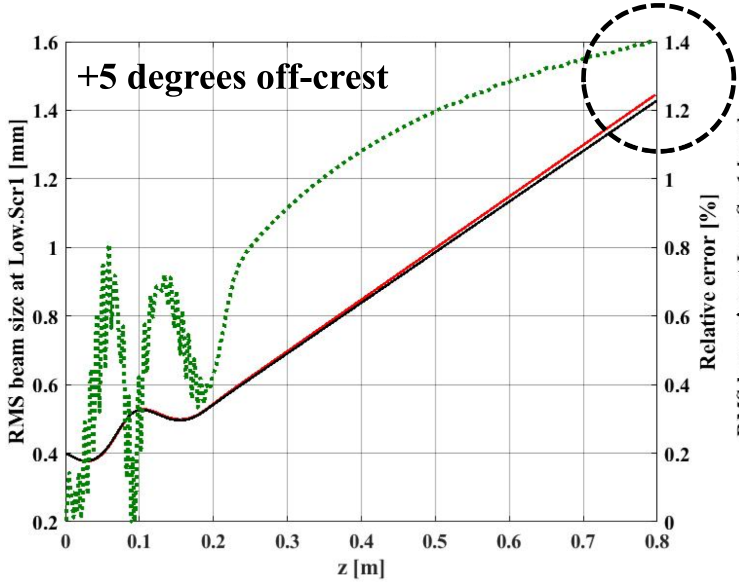

- case of traveling wave (60.58MV/m)
- case of standing wave (59.57MV/m)
- relative error

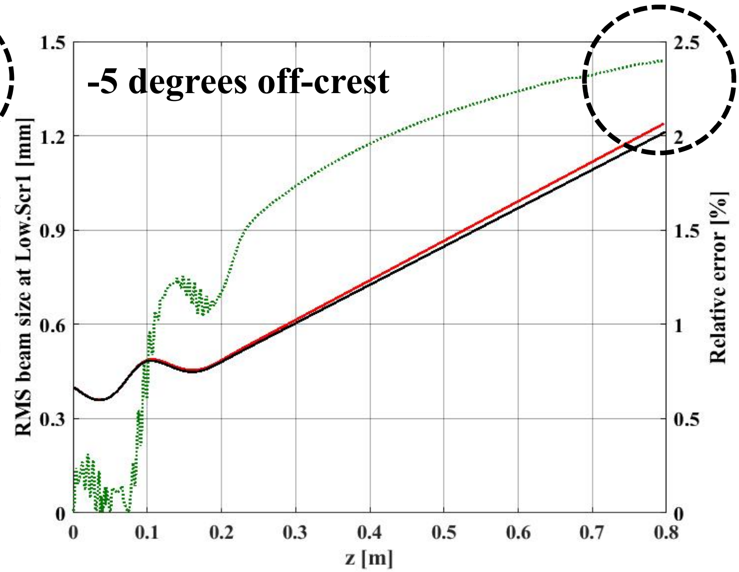

- case of traveling wave (60.58MV/m)
- case of standing wave (59.57MV/m)
- relative error

Comparison of beam size at the 1st screen after gun (z=0.8m)

Solenoids OFF, RF phase scan

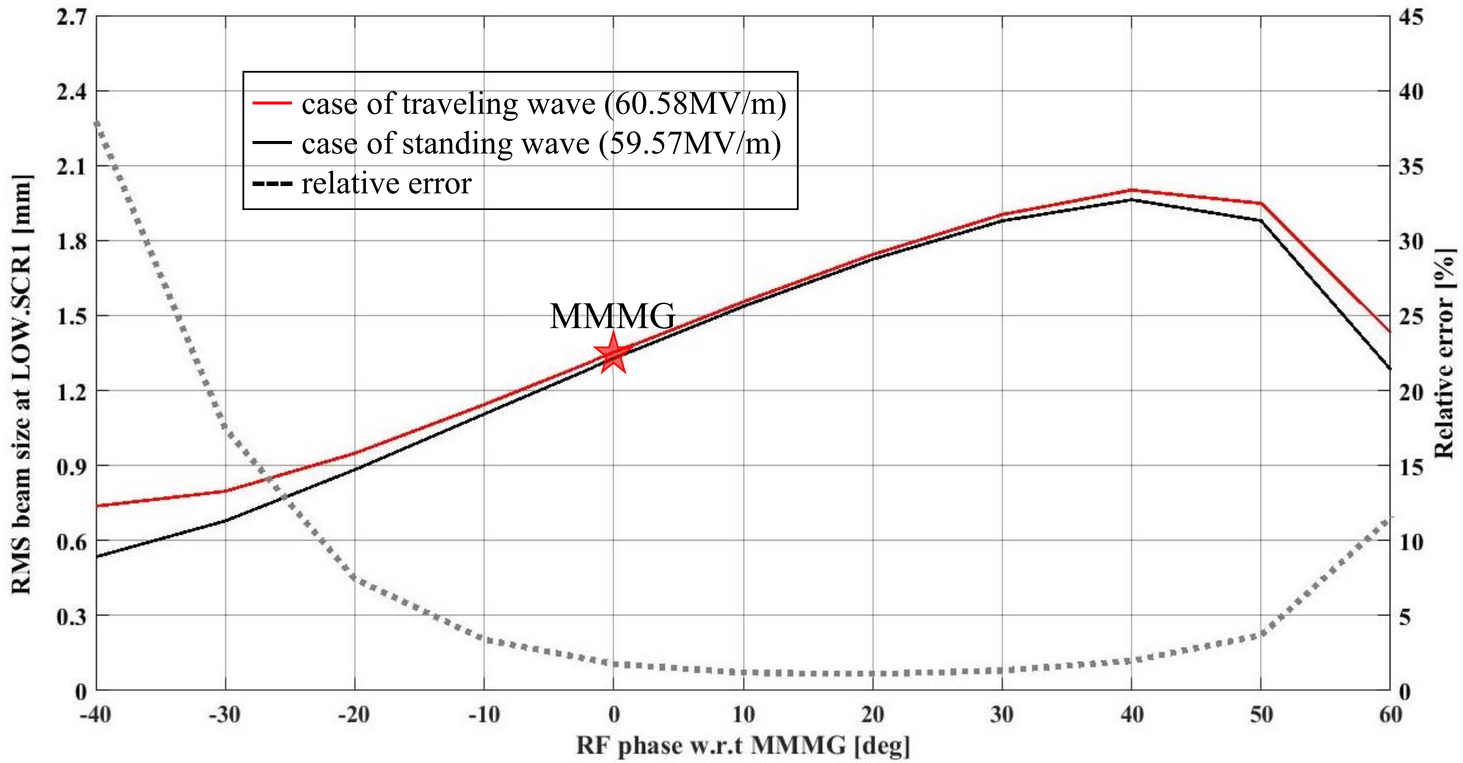

Comparison of beam size with solenoids on

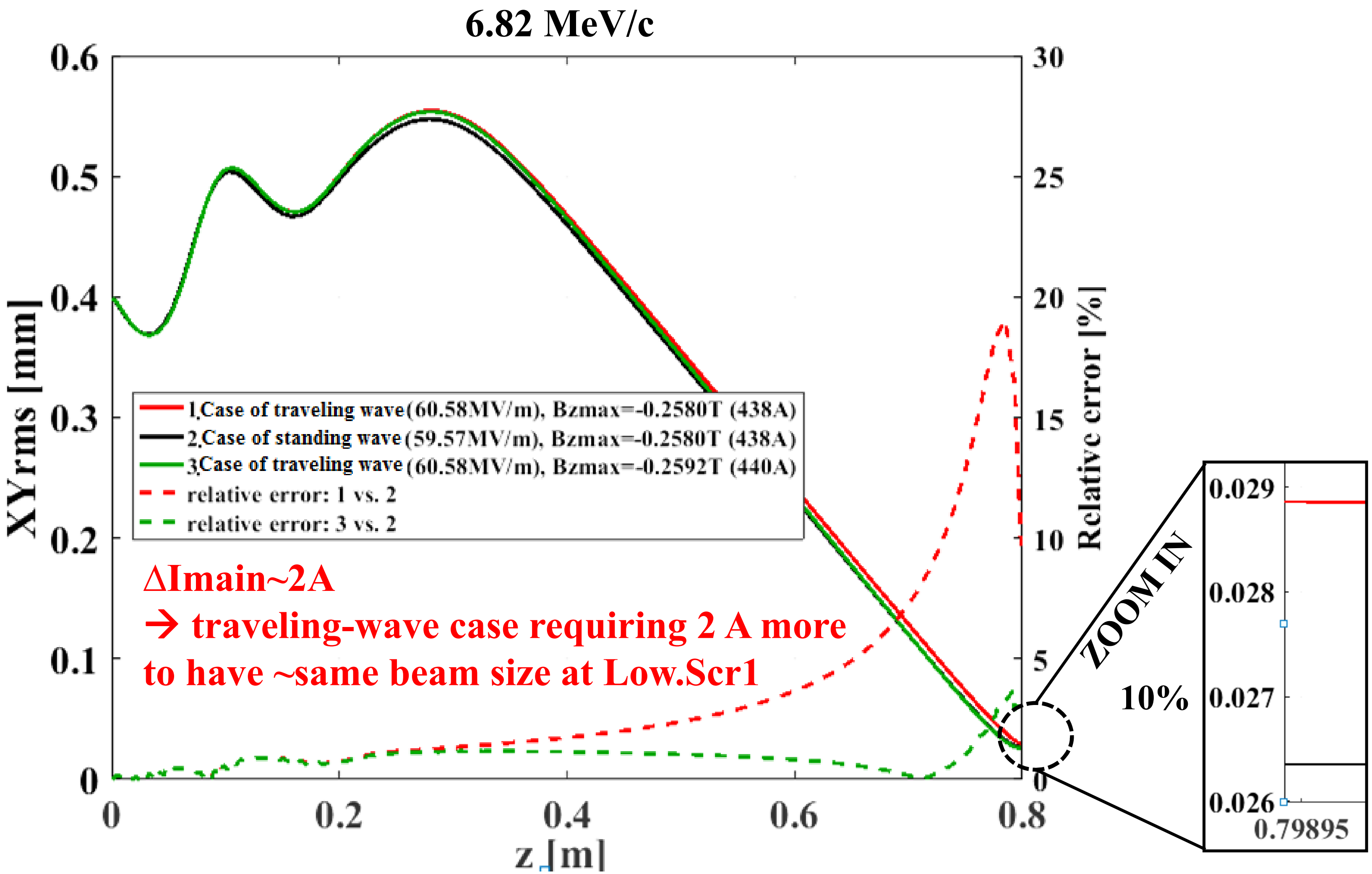

Comparison of beam size by solenoid current scans

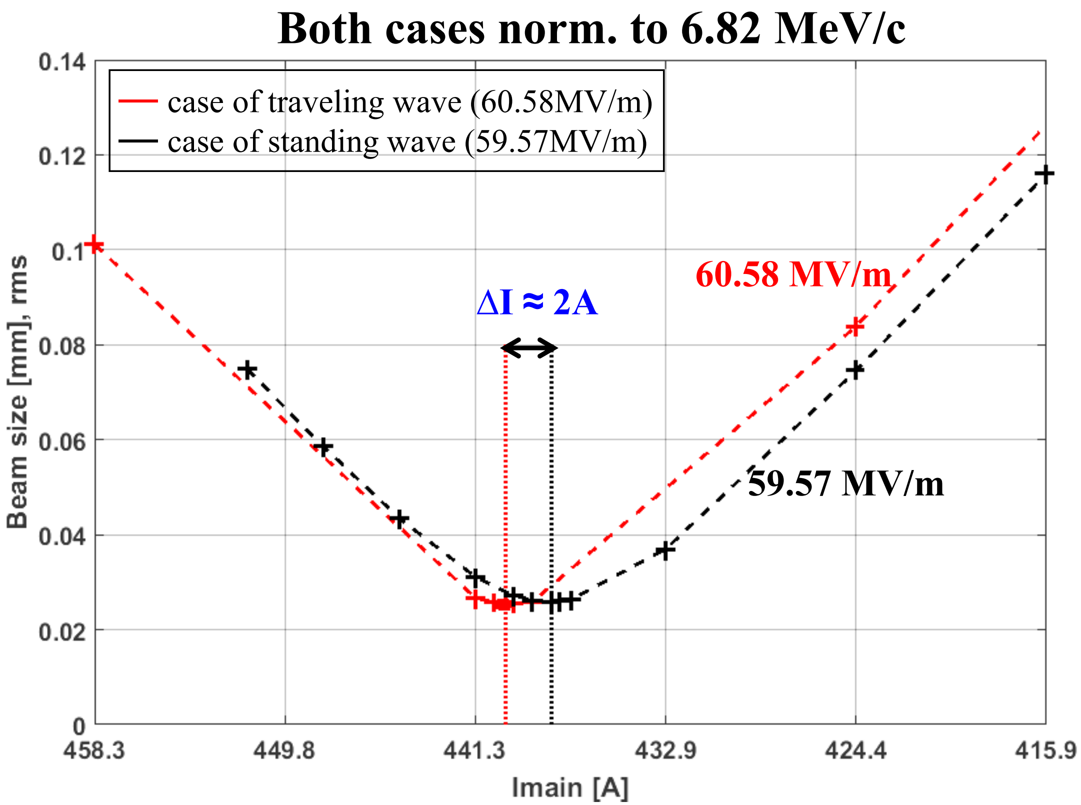

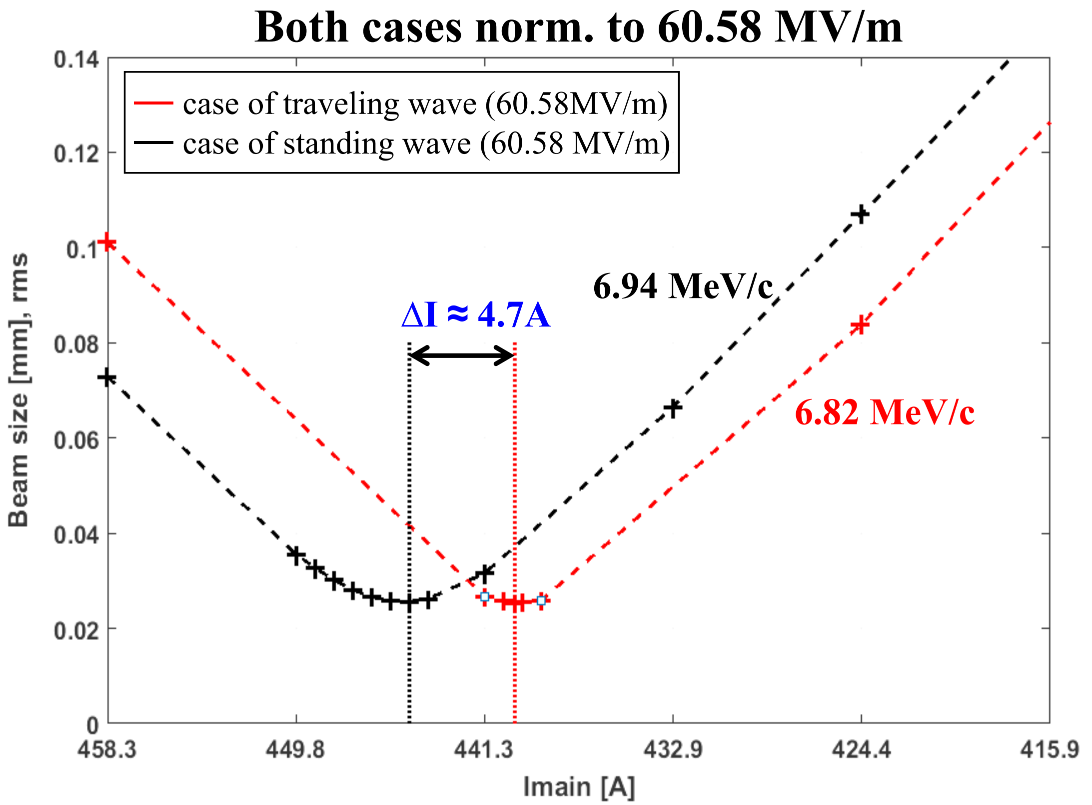

BSA=1.6mm, MMMG, w/o SPCH

Solenoid current scans at 3 screen stations

e-beam momentum: ~5.86 MeV/c

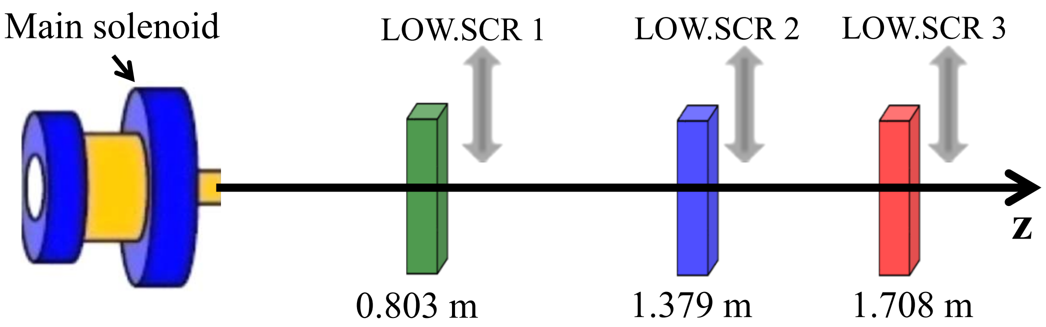

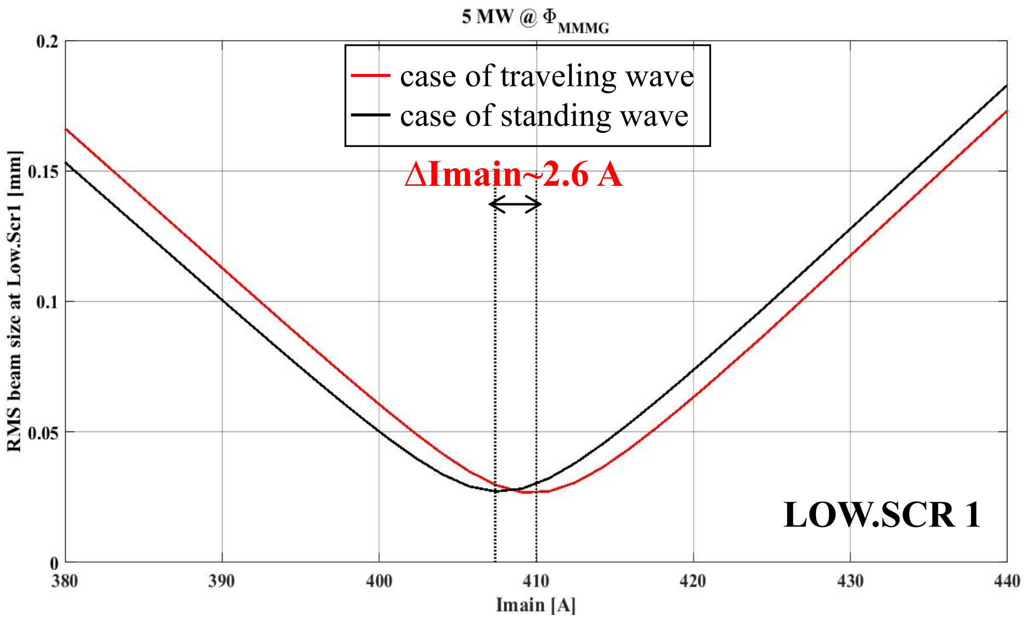

No space charge considered

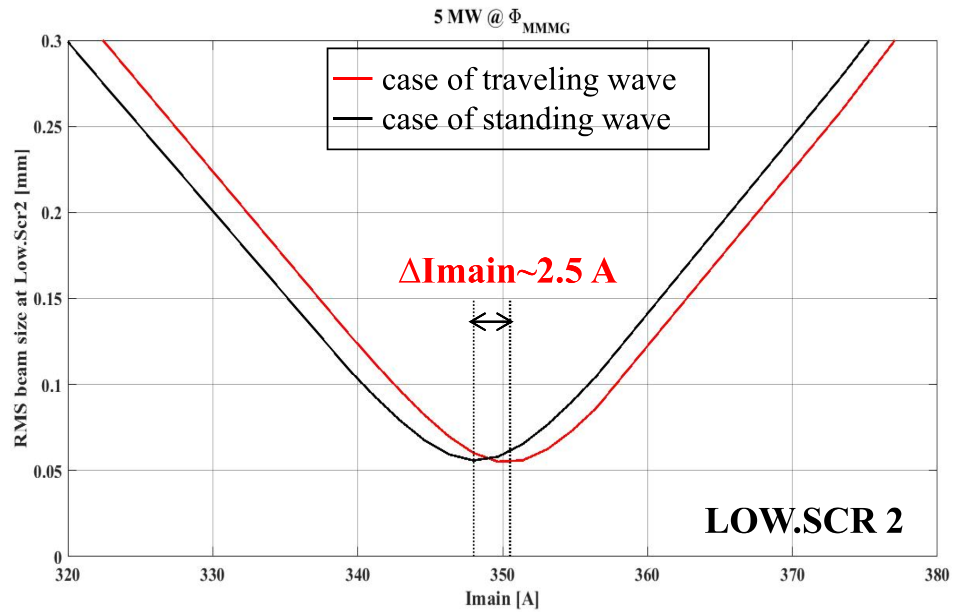

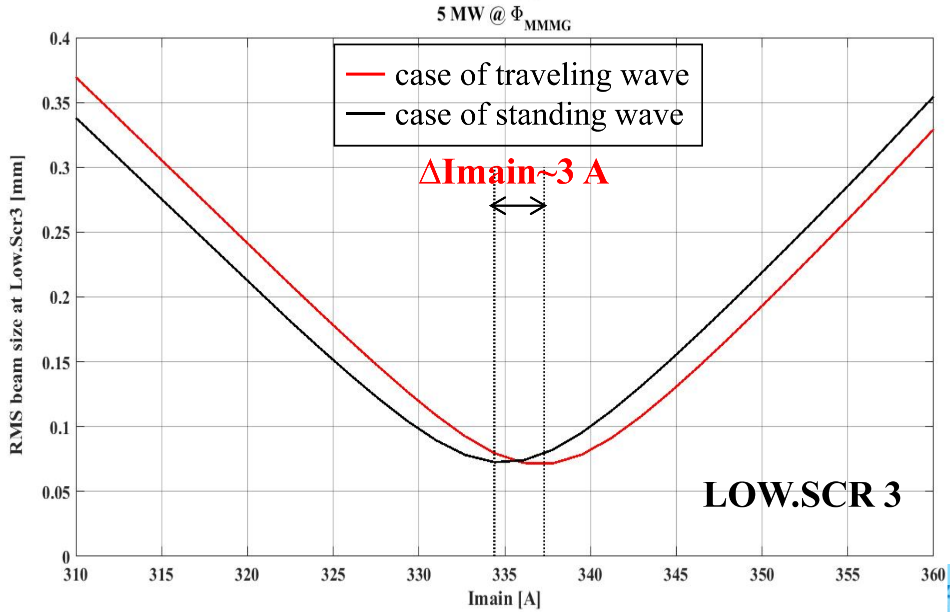

Beam size measurements in low energy section

Measurement setup

RF power

RF2C10MW		code	0
		no pulse	
forward power	6.071 MW	gradient	52.818 MV/m
reflected power	0.049 MW	slope	15.300 dBm/ms
power	5.021 MW	reflection	9.680 %%

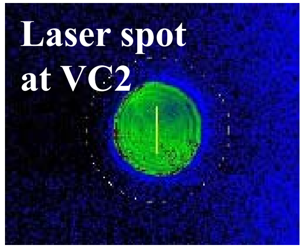

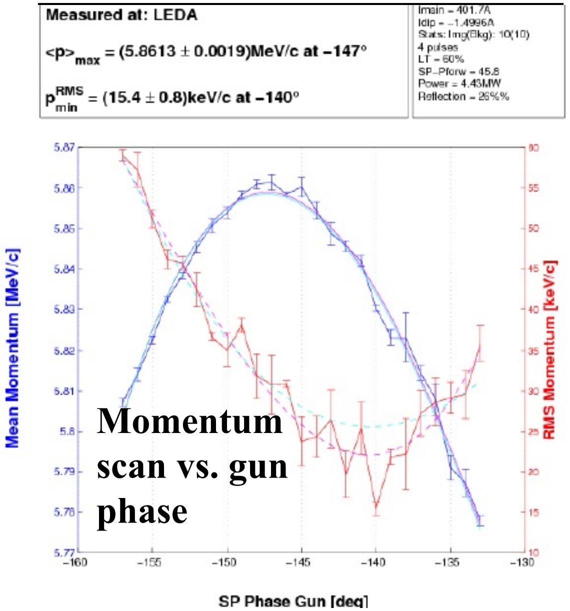

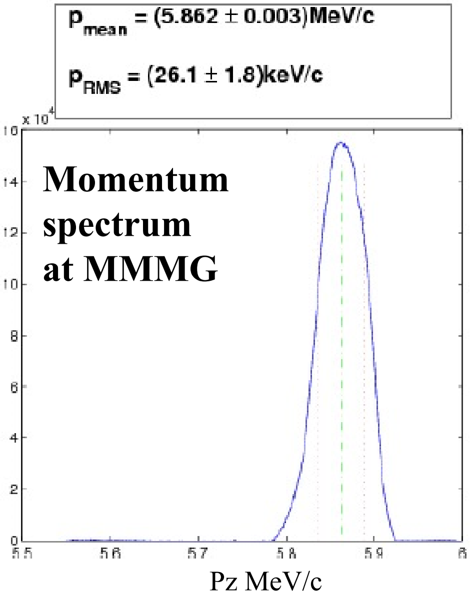

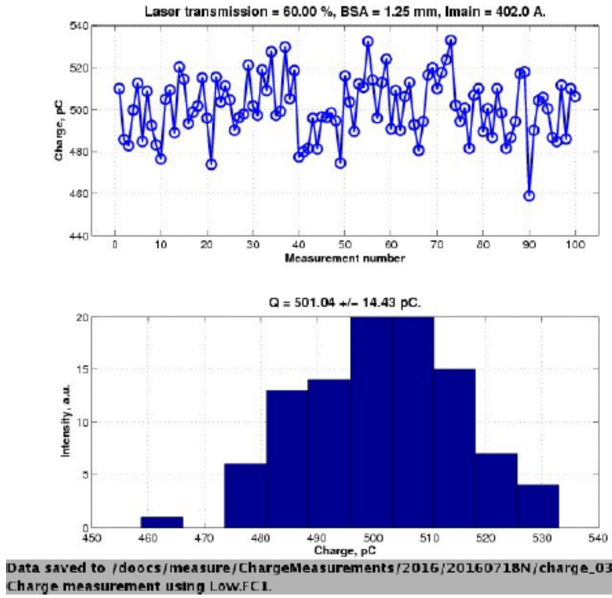

Charge measurement

Measured e-beam size at 3 screen stations vs. solenoid scan + comparisons with standard Astra simulations using Ez profile from Eigenmode

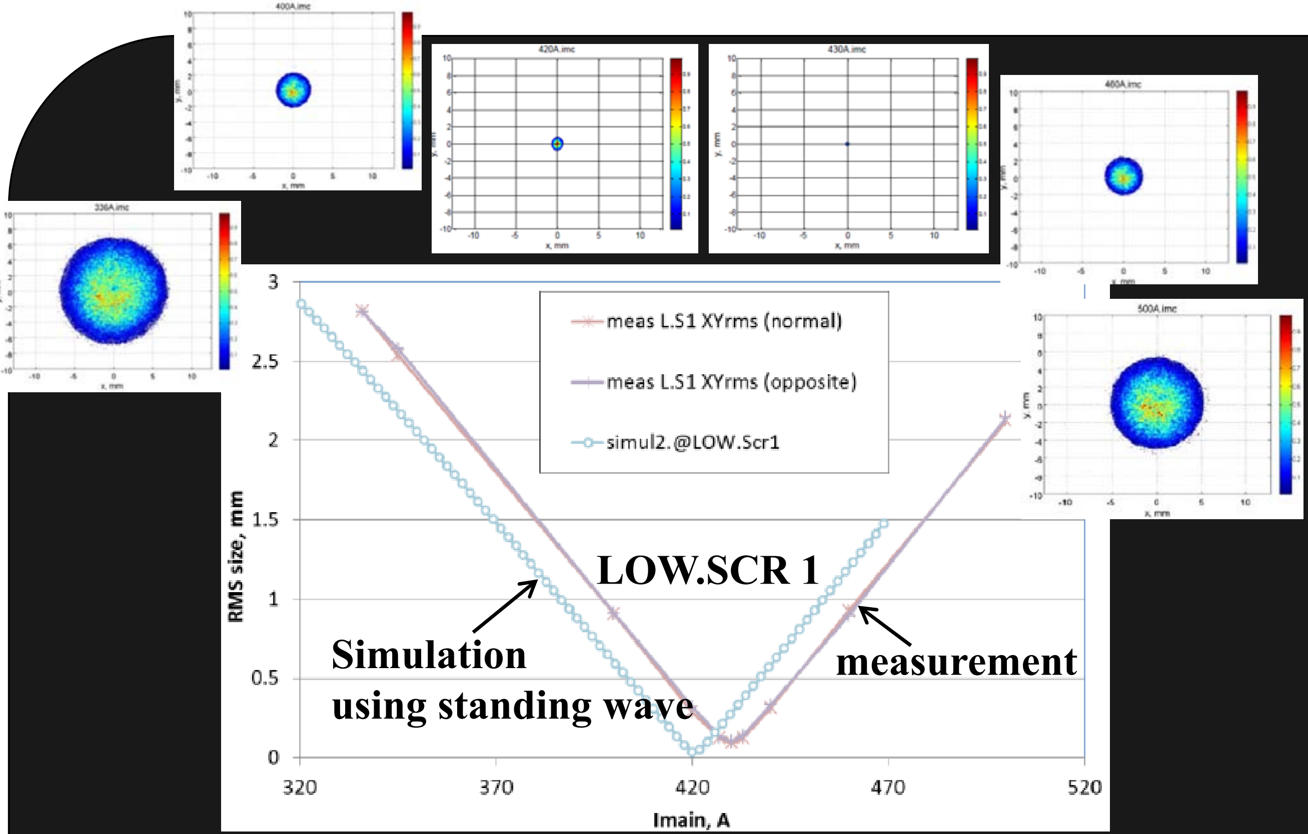

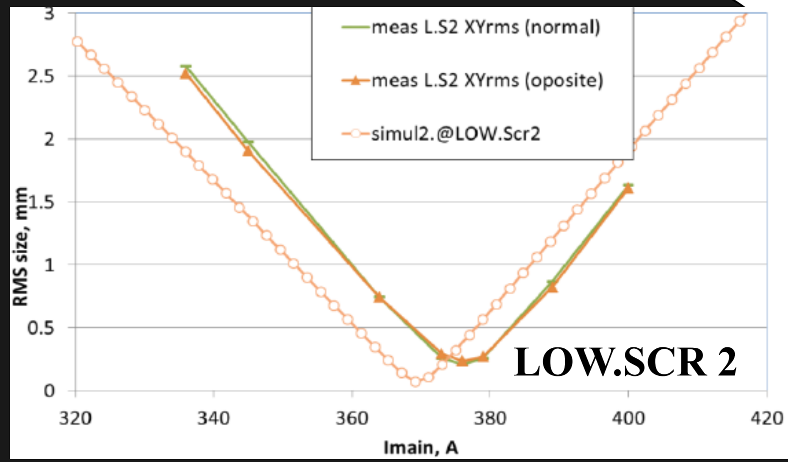

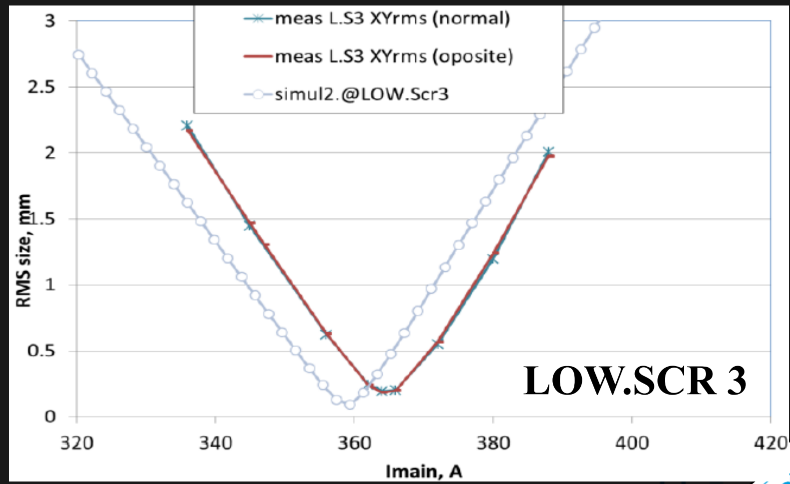

1. ΔImain~6A for measurement vs. simulation (standing wave case)
2. At least ~50% of this discrepancy seems coming from the traveling wave effect by the end of the coaxial line

Influence of space charge (solenoids off)

Space charge making the effect more pronounced

w/o space charge

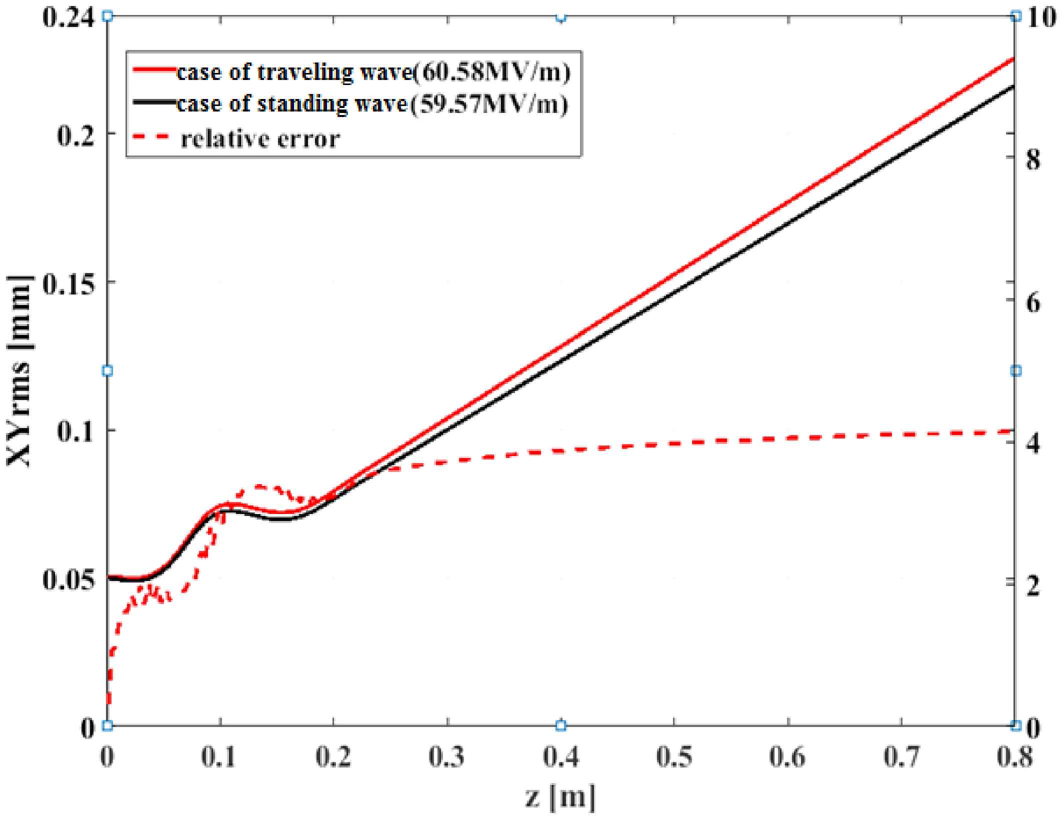

w/ space charge

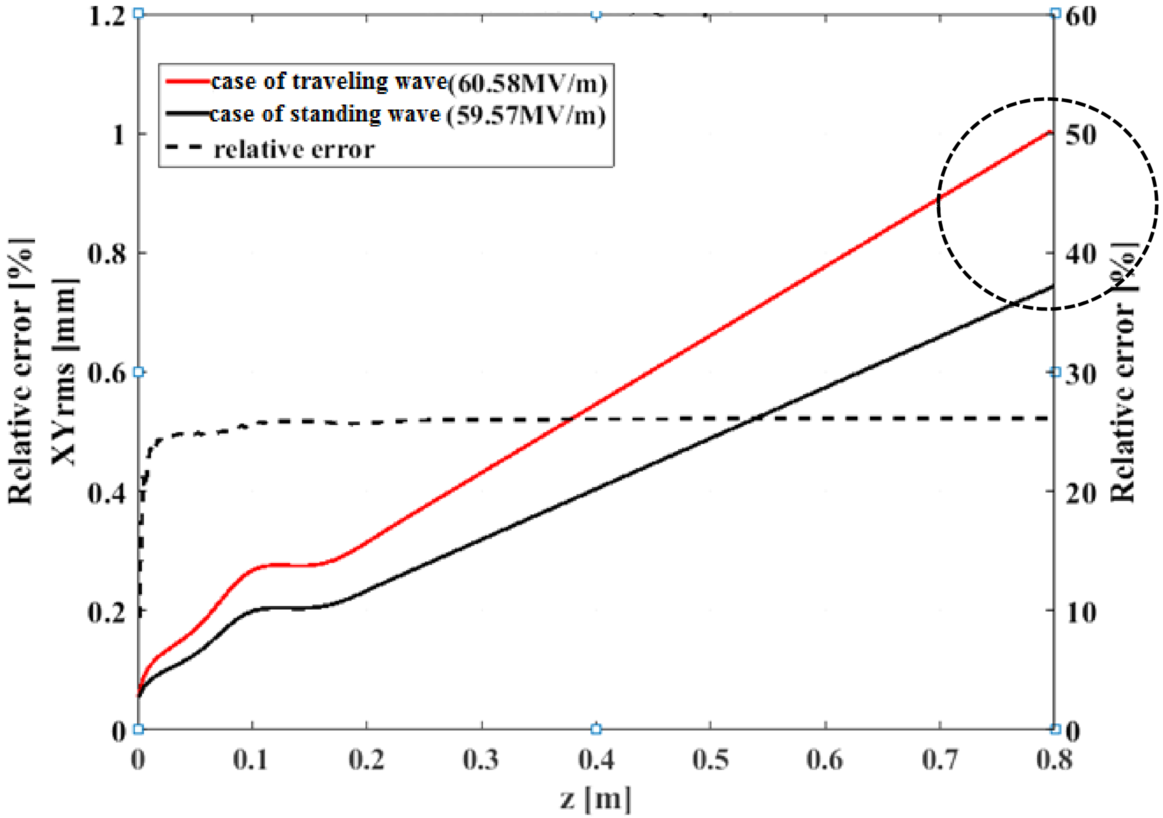

BSA=0.2mm, Q=5pC, MMMG, 6.82MeV/c

Source of discrepancy for beam focusing

1. Field balance
2. Traveling wave in the transition region
3. To identify the main source:

→ Off-axis GeV-particle [x0, 0] (at cathode) tracking

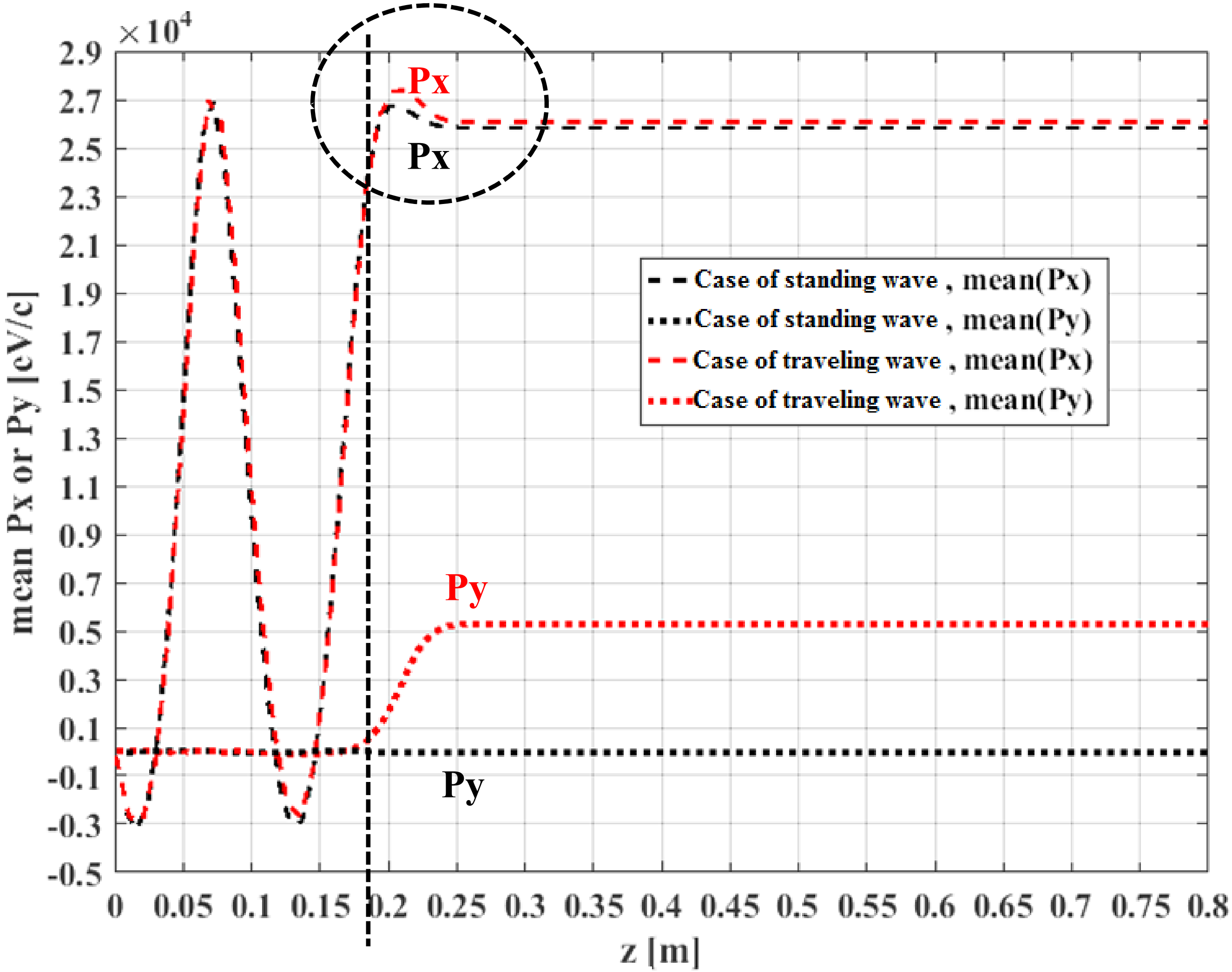

Source of discrepancy for beam focusing

1. **Field balance**
2. **Traveling wave in the transition region**
3. **To identify the main source:**

→ Off-axis GeV-particle [0, y0] (at cathode) tracking

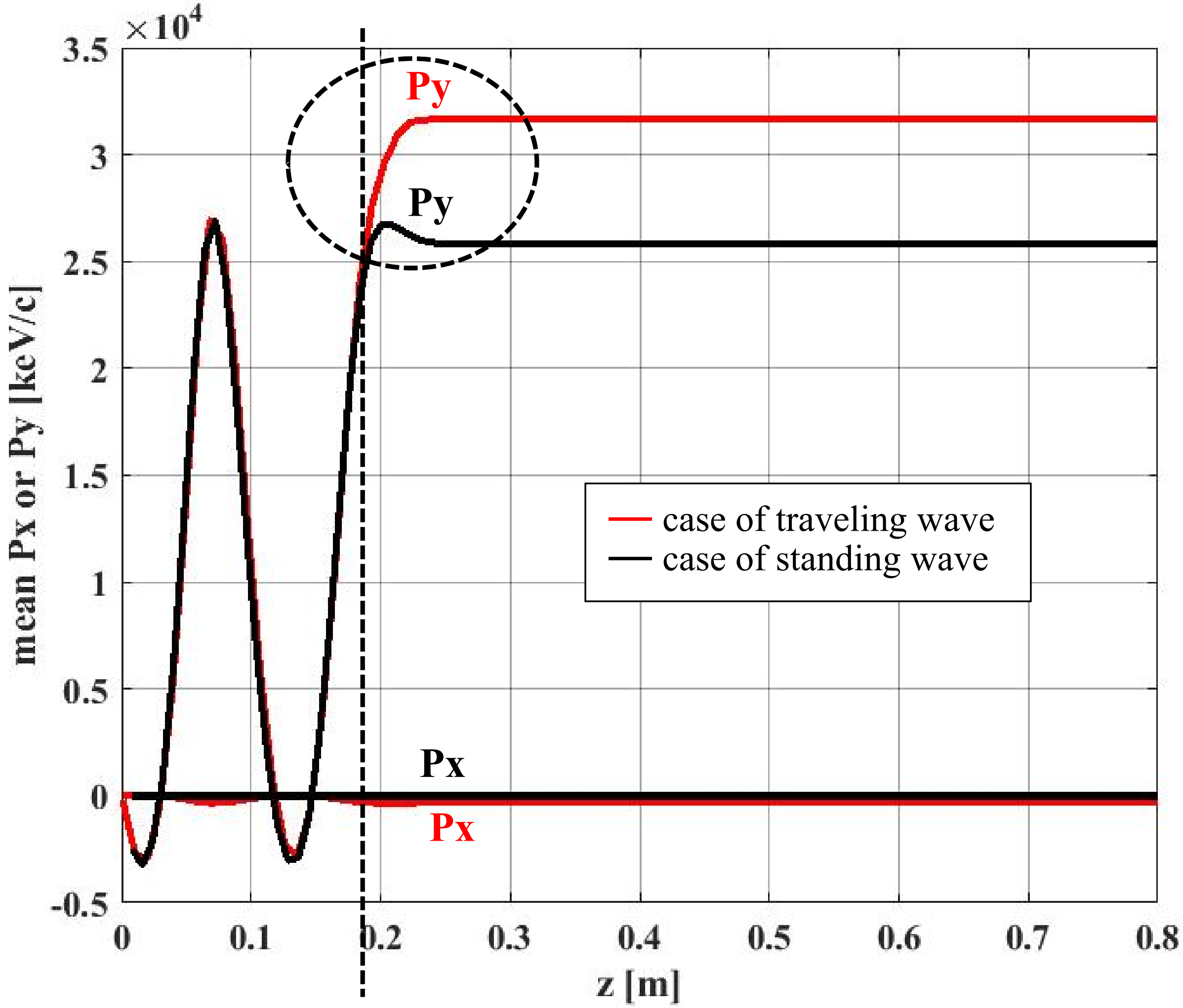

- **→ The traveling effect by the end of the coaxial line affects the beam focusing**
- **→ Partially explaining ΔImain between measurement and simulation**
- **→ RF focusing not obviously affected**

Laser Beam Based Alignment (BBA)
— motivation / introduction

- Putting beam to beamline center
- Measurements affected by RF focusing and kick → impacts?
- Principle
  - The **radial** component of the **RF field** on the **axis of symmetry** identically equal to **zero**
  - If the electron moving along the axis sees only the RF field, its **trajectory independent on the RF phase;** For **not-aligned beam** its **trajectory depends on** the **RF phase**

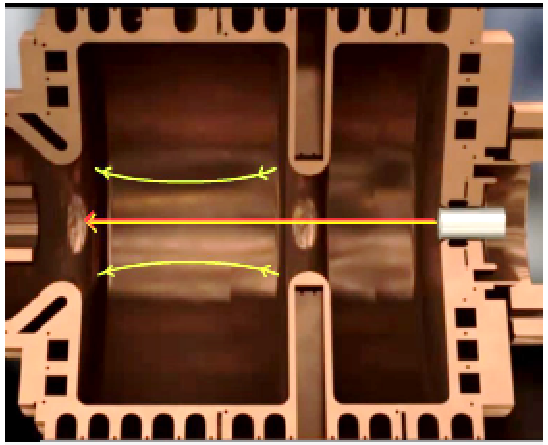

Aligned

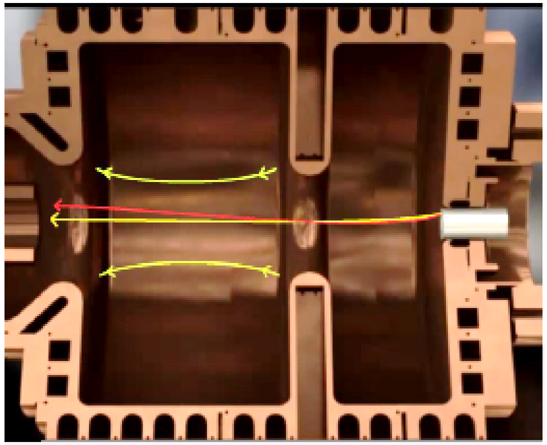

Not-Aligned

Laser Beam Based Alignment (BBA)

- **Conditions and Procedures**

LOW.SCR1

Move laser spot on cathode

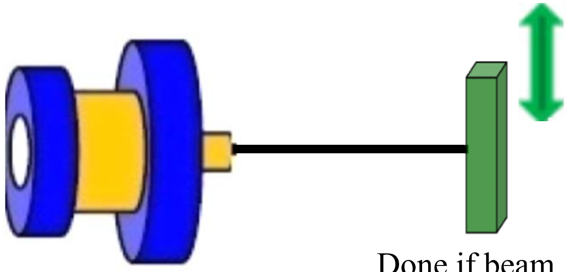

Scan gun phase

Done if beam centroids do not move on screen

- All magnets off
- Use off-crest bunch
- Low RF power level (e.g., 1.5 MW)
- Low charge (e.g.,10 pC)
- Observation screen LOW.SCR1, z~0.8m

+ 3D traveling-wave field map for simulations

Move laser spot on cathode

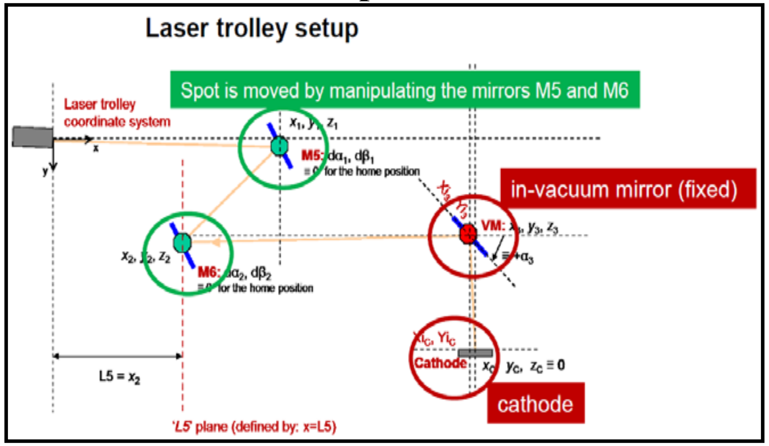

Observe beam centroid position downstream at LOW.SCR1

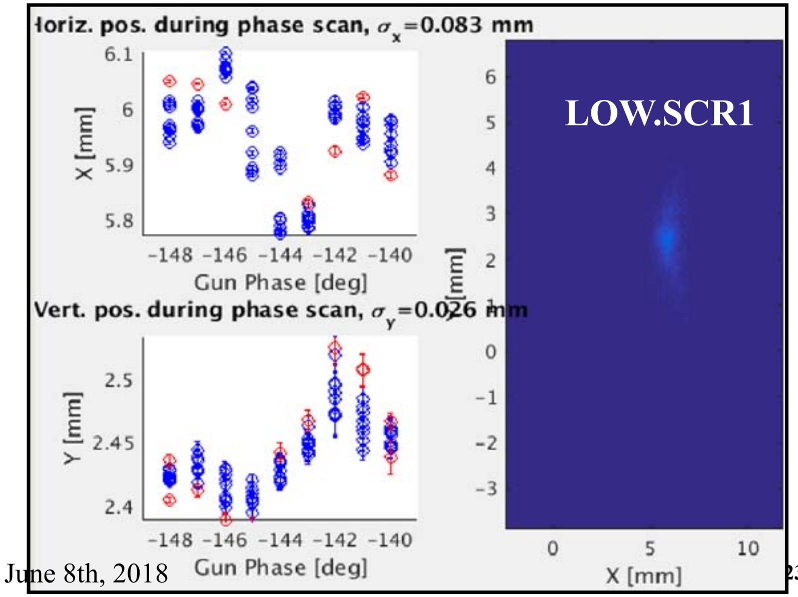

Simulation of Laser BBA at different RF power levels, 1.5 MW vs. 6.5 MW

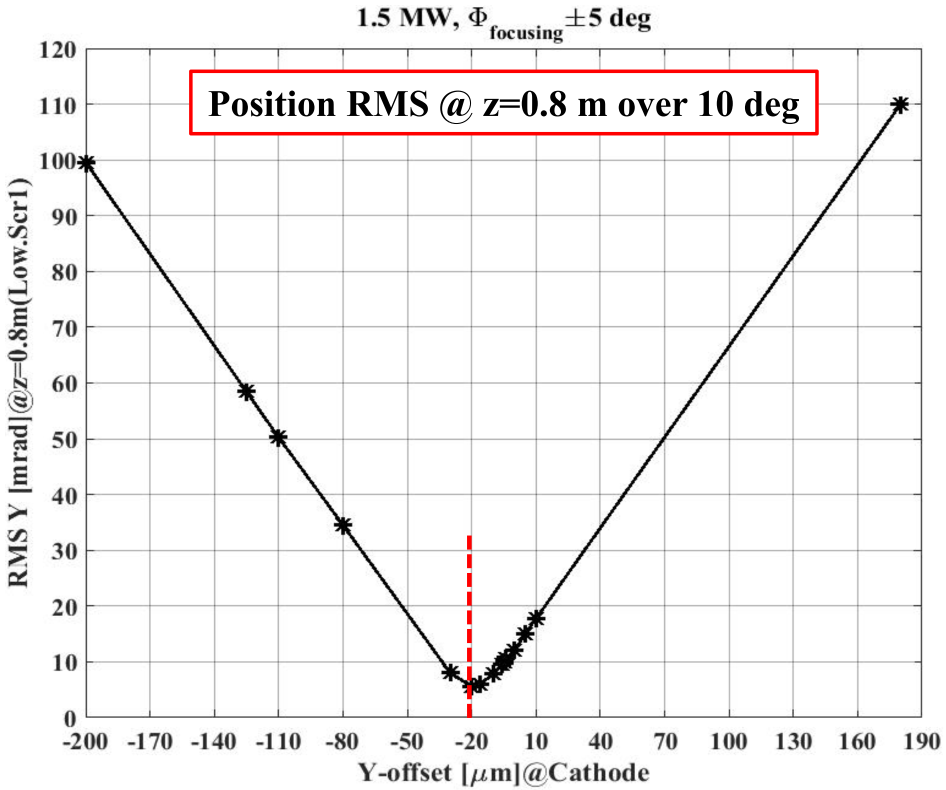

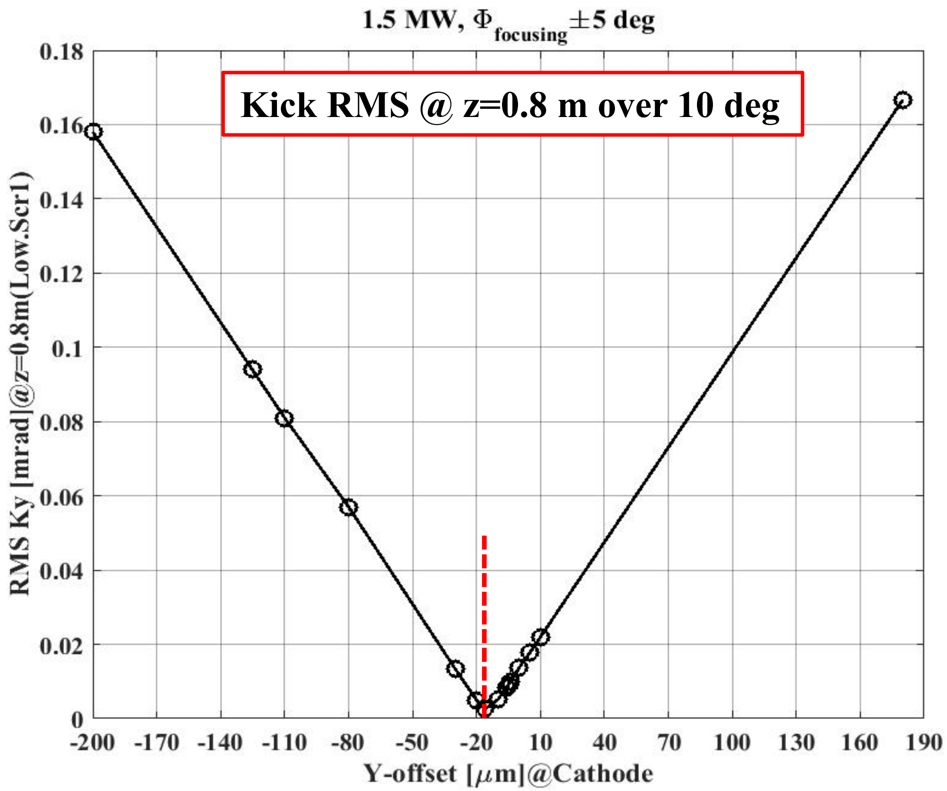

$\Phi_{focusing}$: RF (best) focusing phase

Ky = Py/Pz, **momentum change cannot be measured at Low.Scr1**

Low.Scr1: first observation screen after gun, z=0.8m

Simulation of Laser BBA at different RF power levels, 1.5 MW vs. 6.5 MW

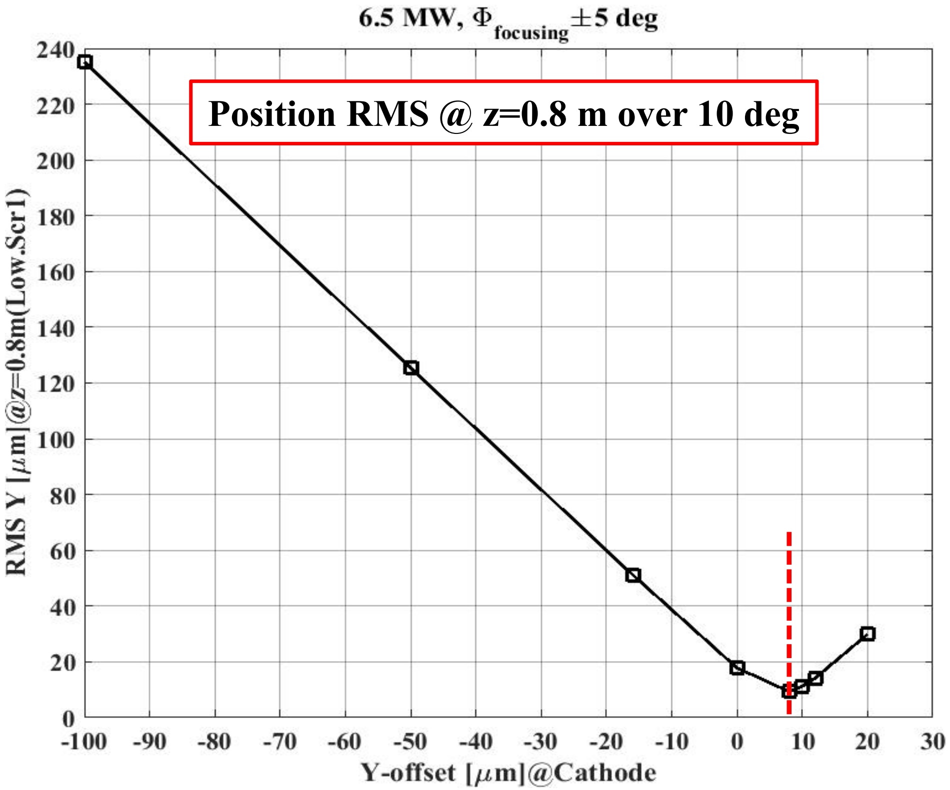

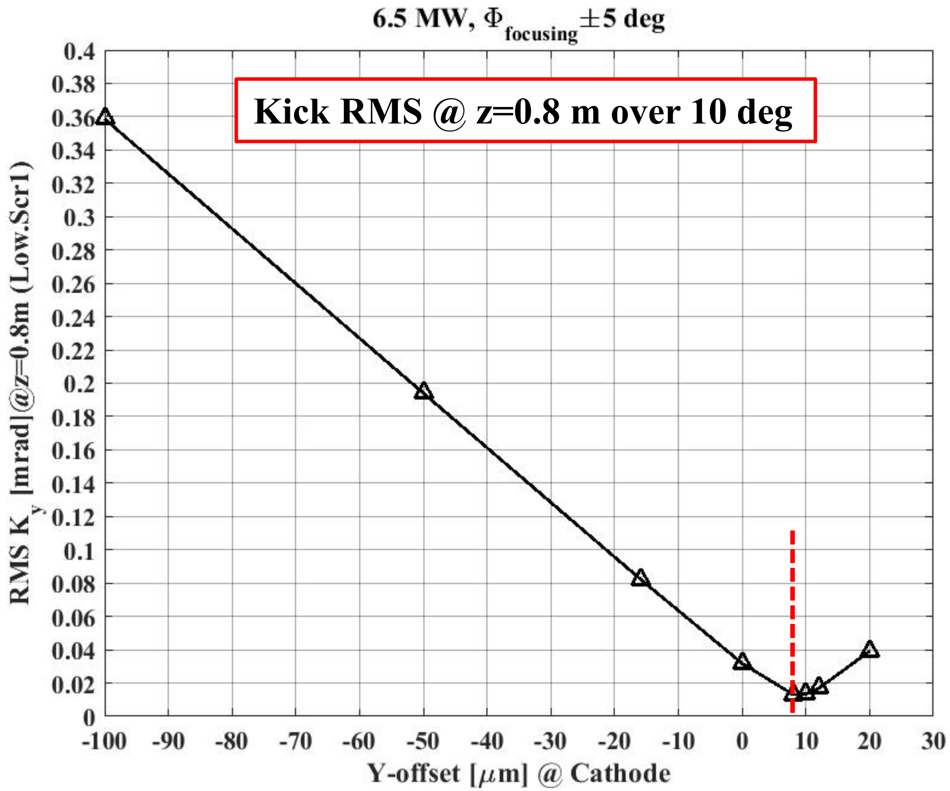

$\Phi_{focusing}$: RF (best) focusing phase

Ky = Py/Pz, **cannot be measured at Low.Scr1**

Low.Scr1: first observation screen after gun, z=0.8m

1. At the same power level, looking at position change or momentum change at LOW.SCR1 not making a big difference
2. At different power levels, BBA may be not giving same results…

Laser BBA at 1.5 MW for nominal operation at 6.5 MW

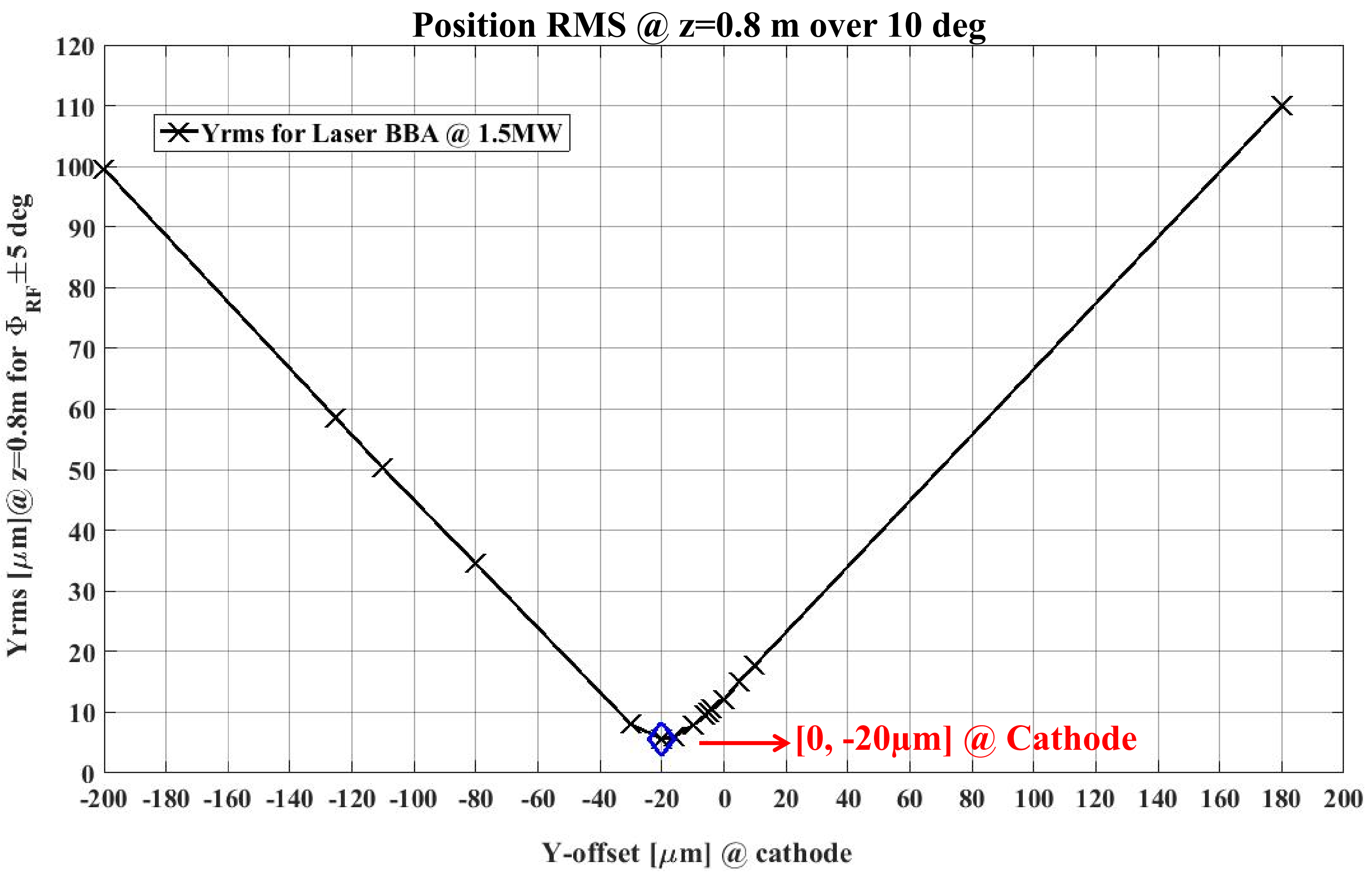

Laser BBA at 1.5 MW for nominal operation at 6.5 MW, Φ_{MMMG}

[0, -20µm] at cathode → kick slope over MMMG±5 deg at the kick location

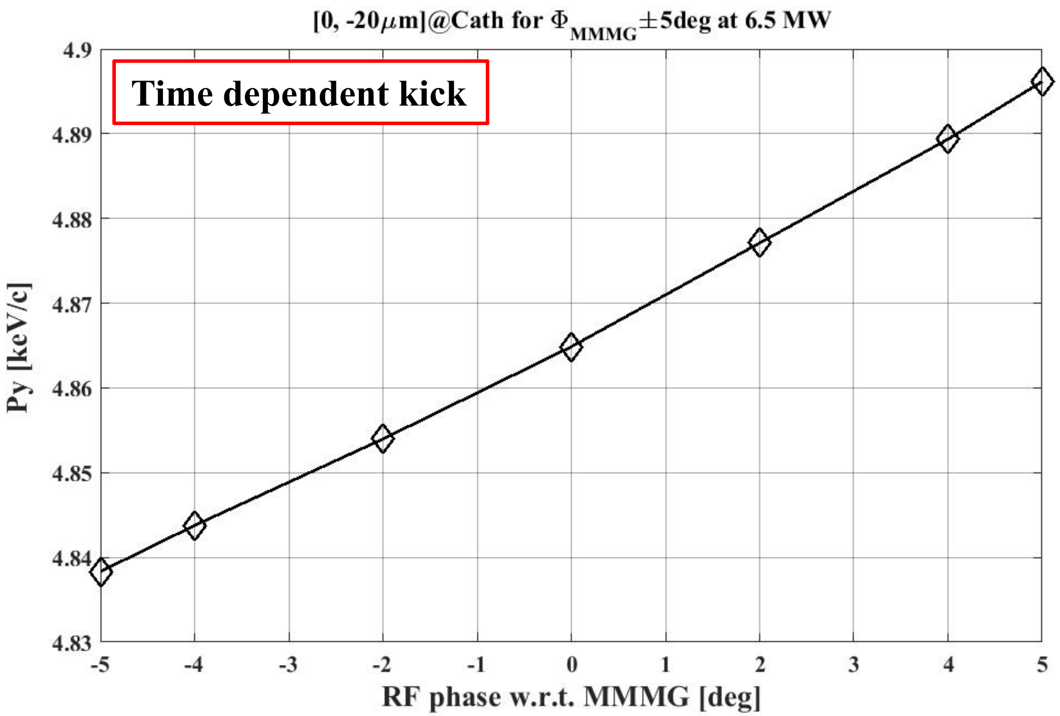

$$\varepsilon_{100\%} = \sqrt{{\varepsilon^2}_{slice} + \Delta\varepsilon^2}$$

e.g., $\Delta\varepsilon^2 \approx {\Delta\varepsilon^2}_{mismatch} + {\Delta\varepsilon^2}_{misalign}$

$$\Delta P_y = 0.005753\Phi$$

σ_y~1.8 mm @ integral kick location for BSA=1.3 mm, 20 ps flattop 500 pC bunch

$$\Delta\varepsilon_y = \frac{0.005753\sigma_\Phi}{mc}\sigma_y \approx \mathbf{0.06\ \mu m}$$

→ Beam position at cathode found by laser BBA approach at 1.5 MW still causing emittance growth at 6.5 MW

→ **IF**, experimental **resolution < ~10 µm**, emittance growth is small at the kick location (~0.2 m), however, it **may get worse downstream** the beam line

Φ_{MMMG}: MMMG phase of the gun

10 degree phase range → ~20 ps electron bunch

"resolution" referring to minimum of Yrms @ Low.Scr1 in experiments

Experimental resolution based analysis on kick slope

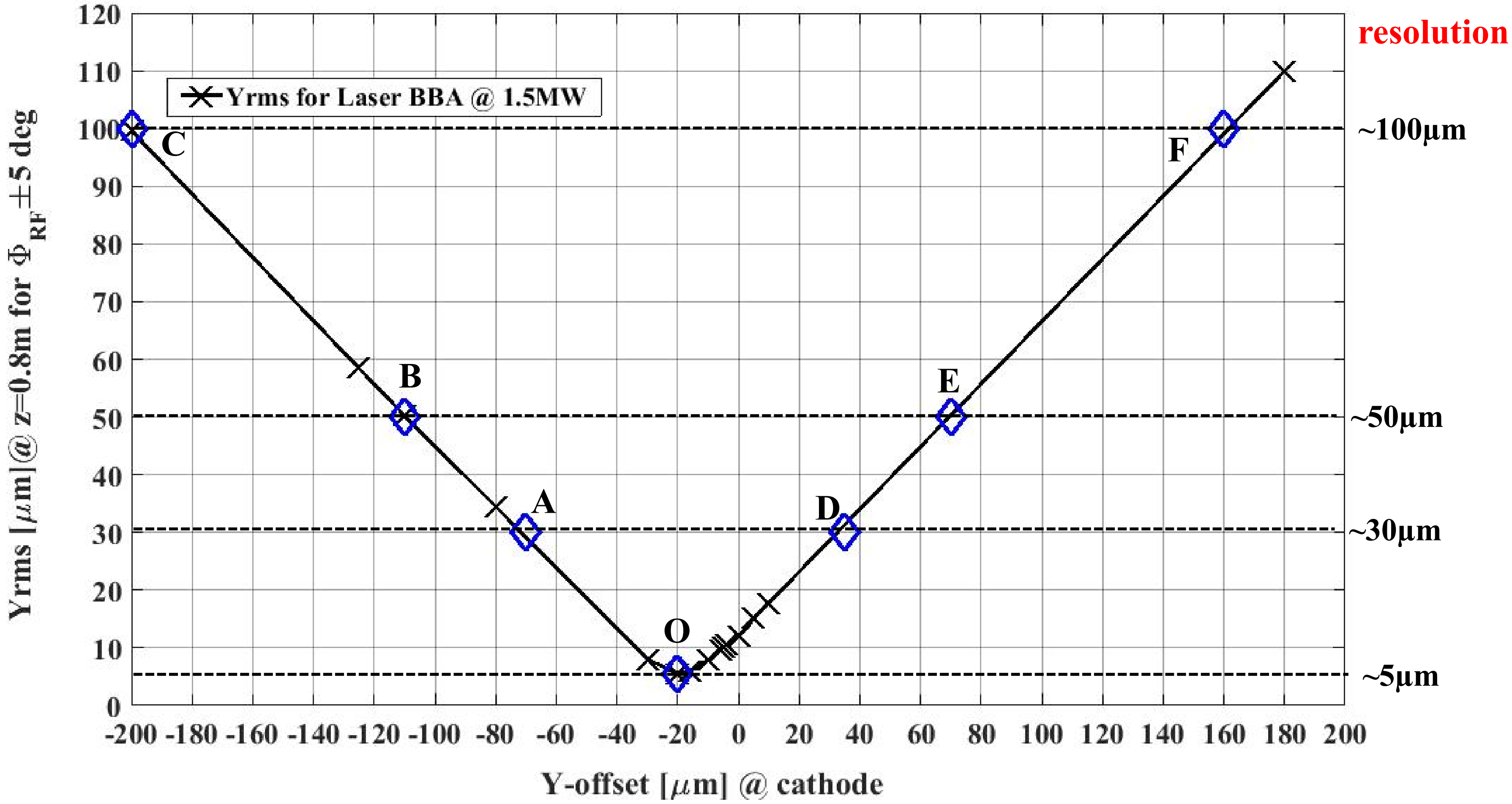

Experimental resolution based analysis on RF kick slope

BBA resolution ~30 µm

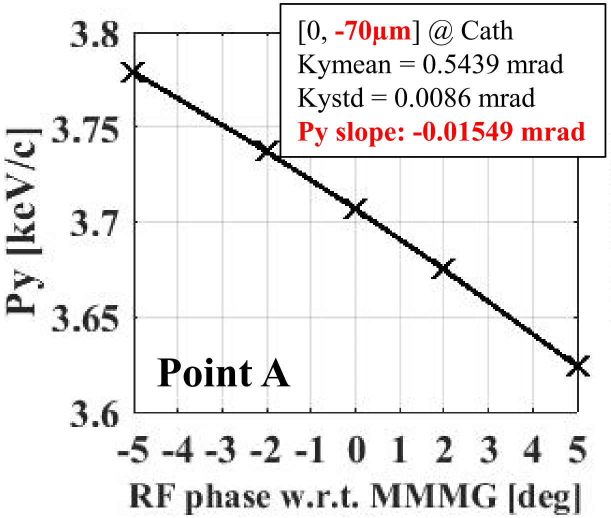

BBA resolution ~50 µm

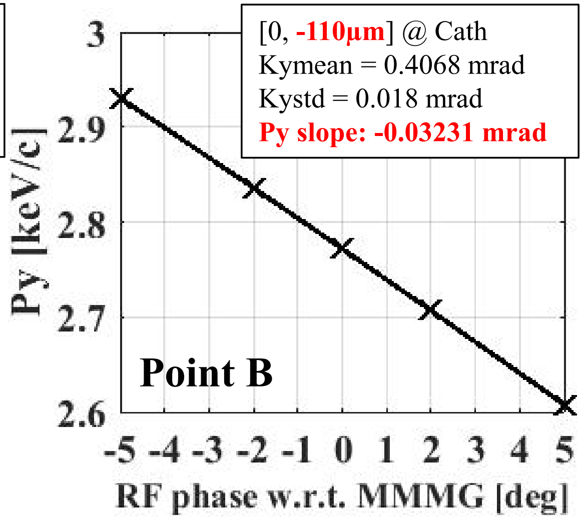

BBA resolution ~100 µm

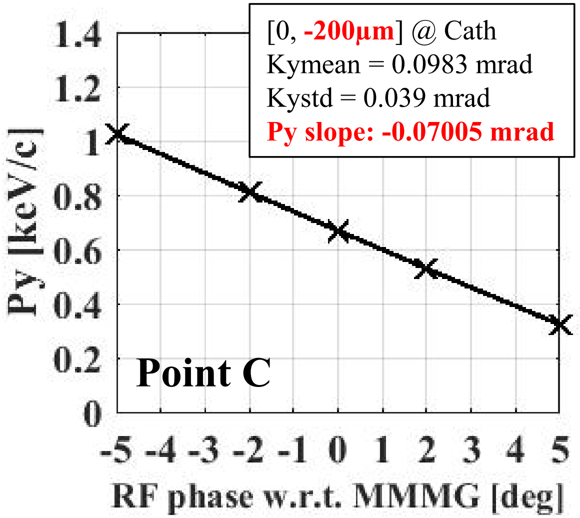

BBA resolution ~30 µm

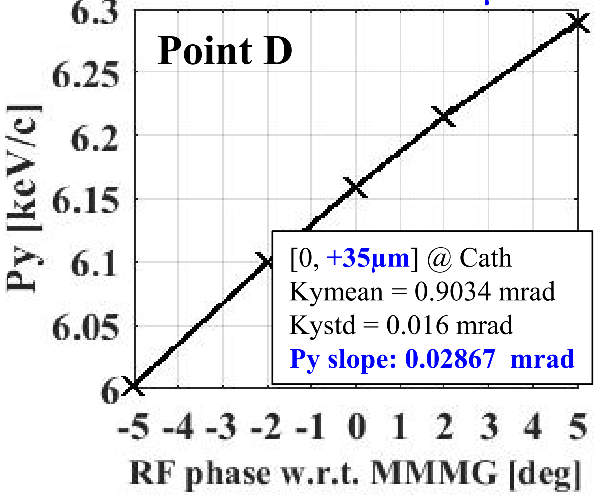

BBA resolution ~50 µm

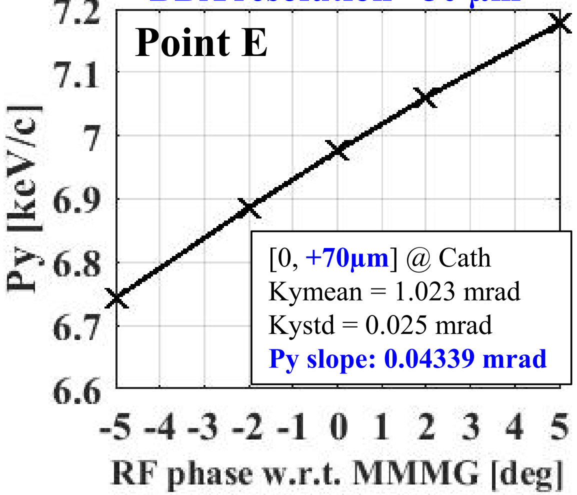

BBA resolution ~100 µm

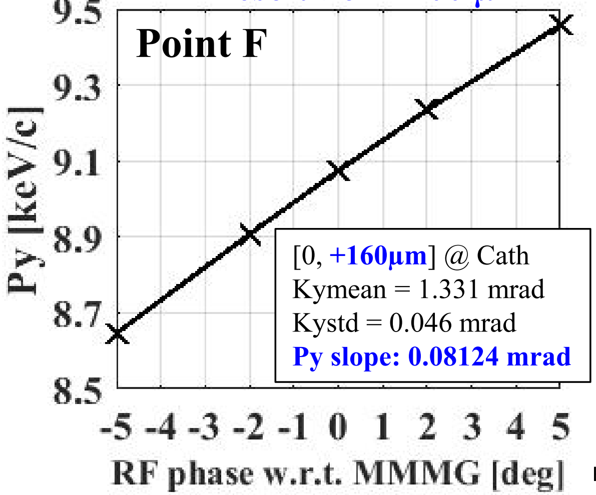

Estimated local emittance growth due to time-dependent RF kick

$$\Delta P_y = K_{slope}\Phi \rightarrow \Delta\varepsilon_y = \frac{K_{slope}\sigma_{\Phi}}{mc}\sigma_y$$

K_{slope}: kick slope, Φ: RF phase, ΔP_y: Y-momentum change

σ_{Φ} : rms RF phase range for a 20ps flattop bunch, $\Delta\varepsilon_y$: Y-emittance growth

σ_y: rms beam size at the integral kick location, **1.8 mm for 500pC (BSA=1.3mm), 2.4 mm for 1nC (BSA=1.8mm)**

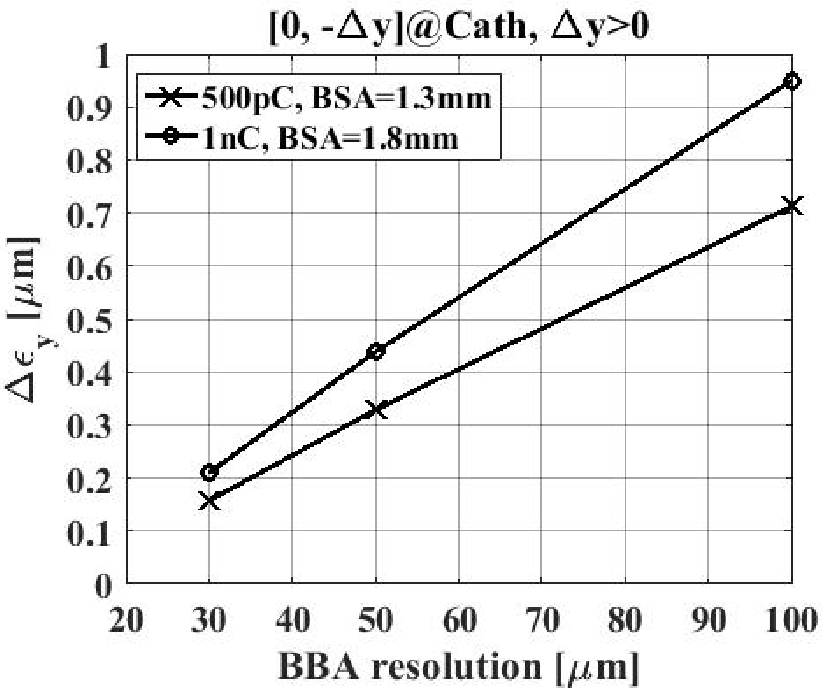

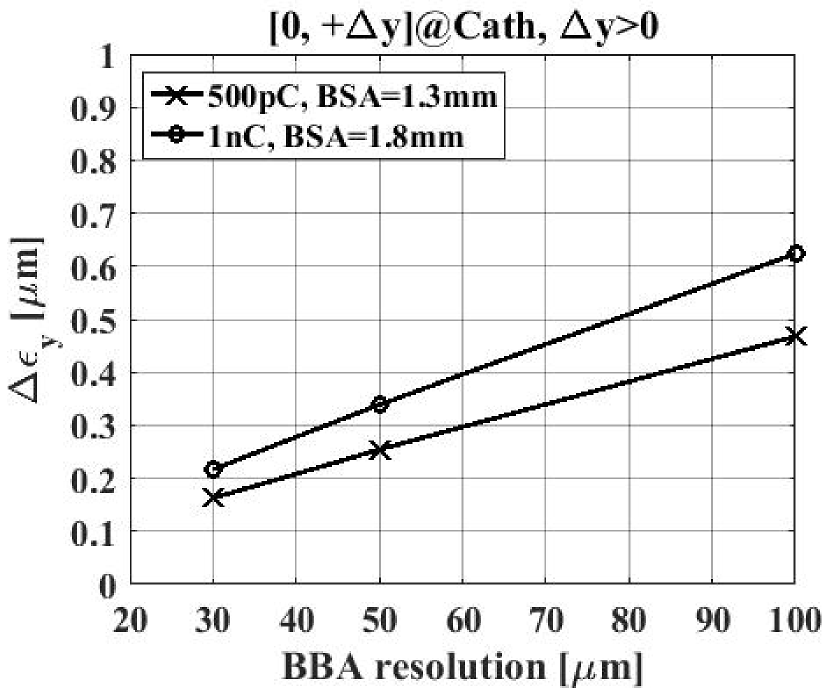

Improved PE modeling approach for photo-gun research
— motivation and status

- Suitable approach for studying **slice emittance formation** in the photocathode vicinity (major part of optimized emittance)
- Potential tool for **photocathode research**

↓

"single particle" emission modeling

→ Not dedicated for gun simulations

→ Not for Cs2Te either

→ **Collective** effects (e.g., space charge) during photoemission not considered

→ **QE not related to space charge**, the latter depends on operation conditions

- **Space charge field impacts** on QE

  → **"on"** cathode surface (vacuum side) → lots of work done

  → **"in"** cathode thin film (material side) → **?**

- Our **measure for a sufficient approach** → agreement of simulation with the measurement at PITZ → **remaining issues**

$$\varepsilon_{100\%} = \sqrt{\varepsilon_{slice}^2 + \Delta\varepsilon_{mismatch}^2 + \Delta\varepsilon_{misalign}^2}$$

Projected emittance decomposition

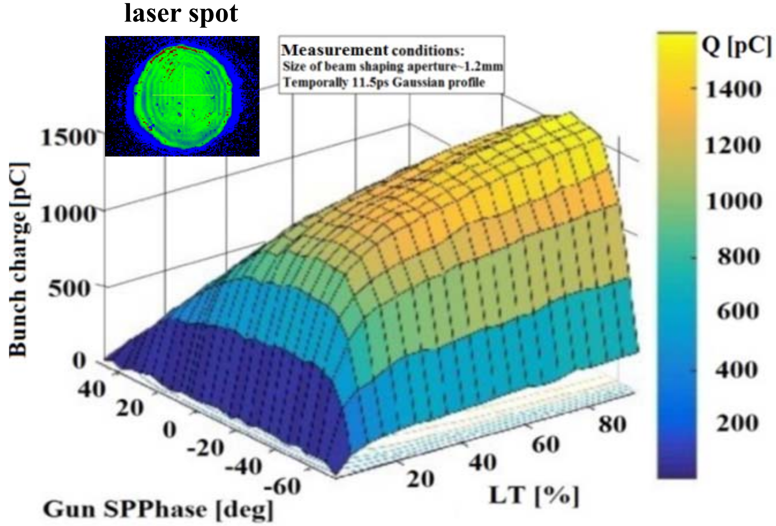

Experimental emission curves at PITZ vs. gun phase and laser intensity

Improved PE modeling approach for photo-gun research — status

Measurements proposed at HZDR:

Emission with **metal cathodes (Mg)** in space charge dominated regime

→ Without considerations of field effects into the cathode thin film, **existing codes and emission modeling work?**

Benchmark 2017
Simulated emission curves with multiple numerical approaches

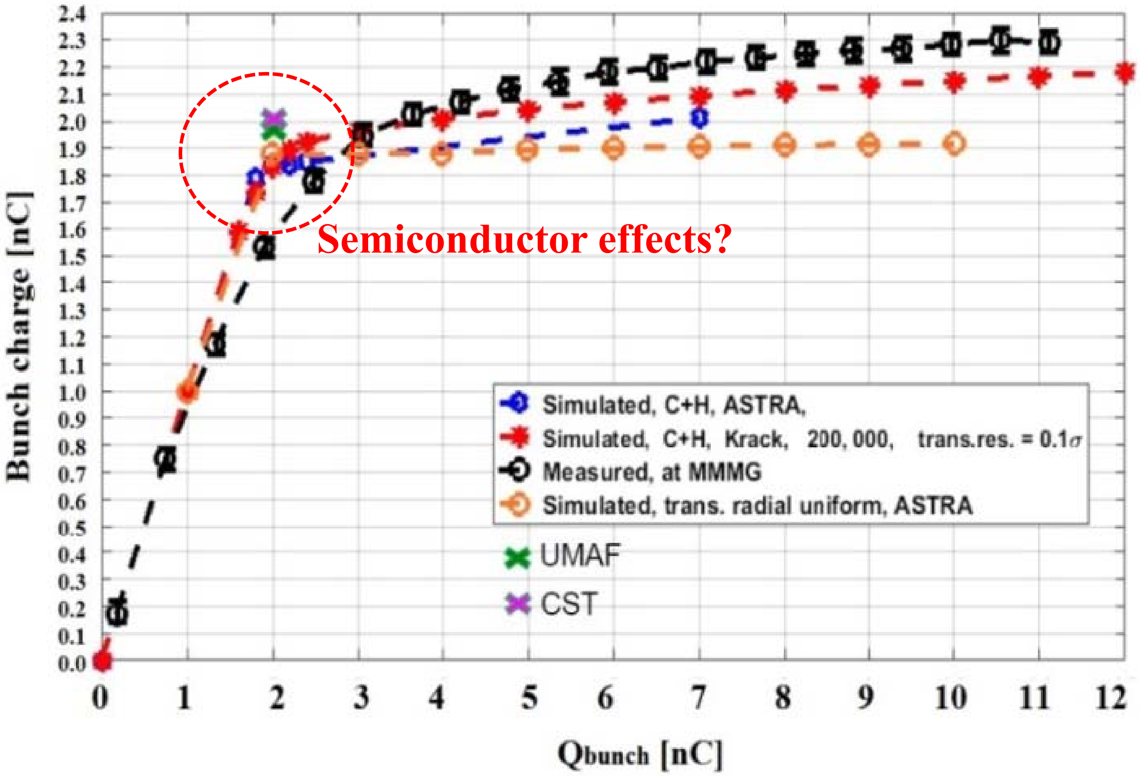

Temporal laser profile

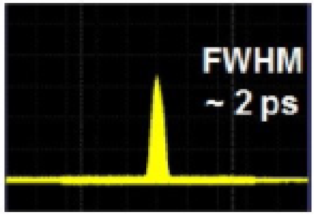

Transverse laser profile

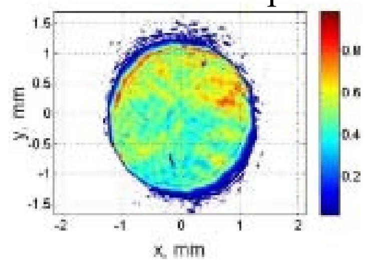

Measurement conditions:

Laser: MBI short Gaussian (2ps fwhm, 0.85ps rms), BSA=2.4mm

RF: Ecath=60 MV/m, Gun @ MMMG

KRACK code: Martin Dohlus
UMAF code: Erion Gjonaj
Simulation results with UMAF provided by Steffen Schmid

Improved PE modeling approach for photo-gun research
— new modeling attempts

1. "Single particle" PE modeling for Cs2Te → based on K. Jensen's work for Cs3Sb
2. Incorporation of space charge effects into "Single particle" emission model

Physical picture of photoemission

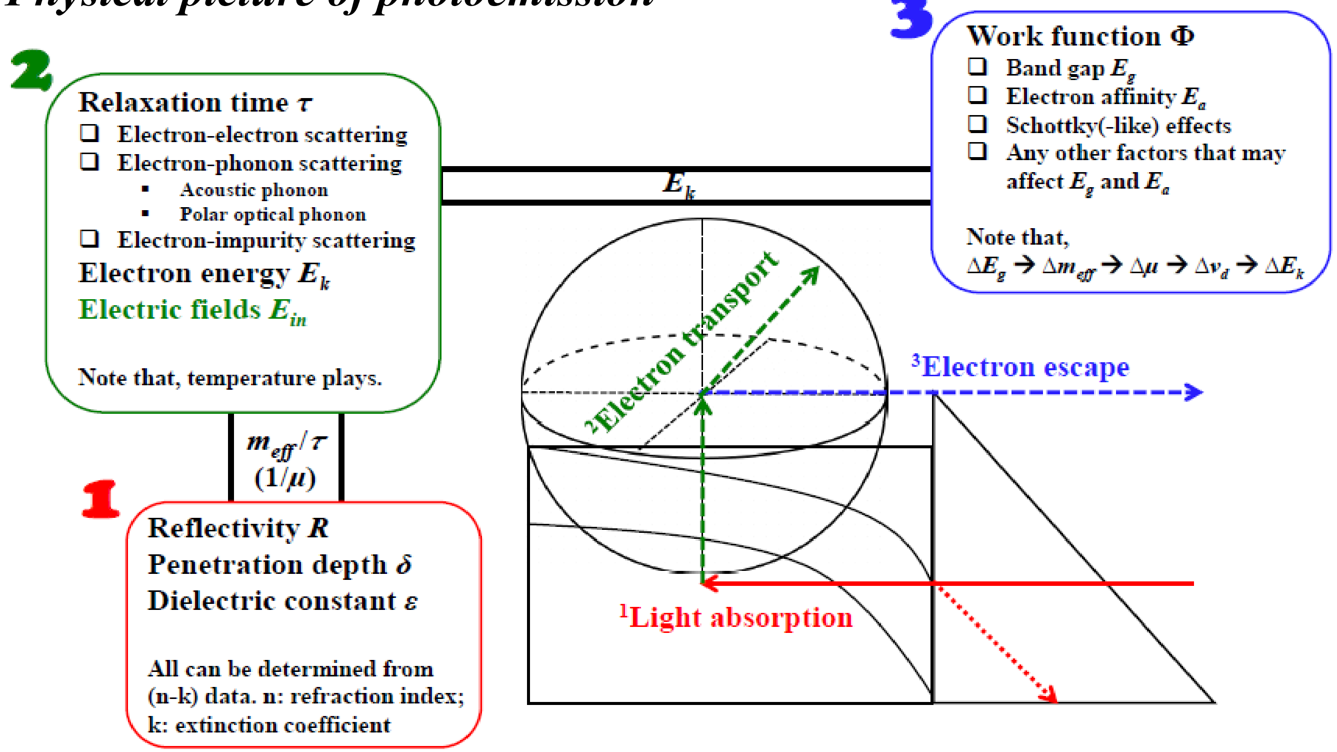

Light absorption in Cs2Te

Refraction index n; Extinction coefficient k; Reflectivity coefficient R; Penetration depth δ; Permertivity ε_r

- ❑ Complex refraction coefficient of materials: $\hat{\boldsymbol{n}} = \boldsymbol{n} + \boldsymbol{ik}$
- ❑ Data* (λ ∈**[250 517]nm**) from sets of reflectivity measurements and dispersive analysis→ $\boldsymbol{n} \in$ **[0.8 1.8];** $\boldsymbol{k} \in$ **[0.3 0.7];**

  → not 1-1 to wavelength

$\boldsymbol{R} \approx \frac{(n-1)^2+k^2}{(n+1)^2+k^2} \in$ **[2.15 14.21]%**

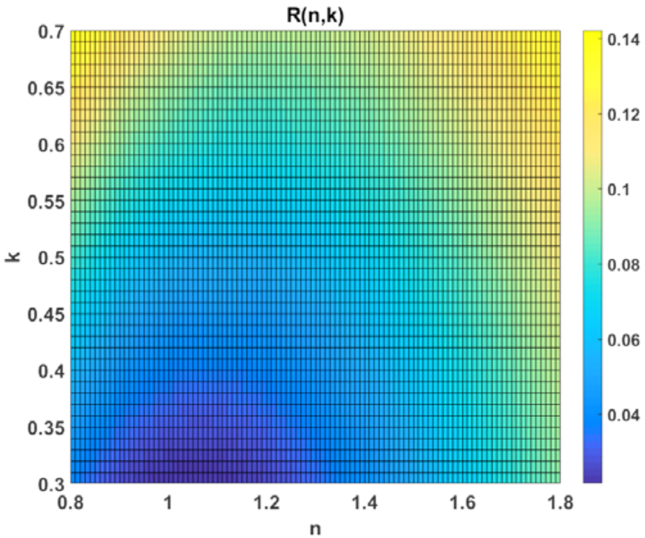

$\boldsymbol{\delta} \approx \frac{\lambda}{4\pi k} \in$ **[29 68]nm**@ 257 nm

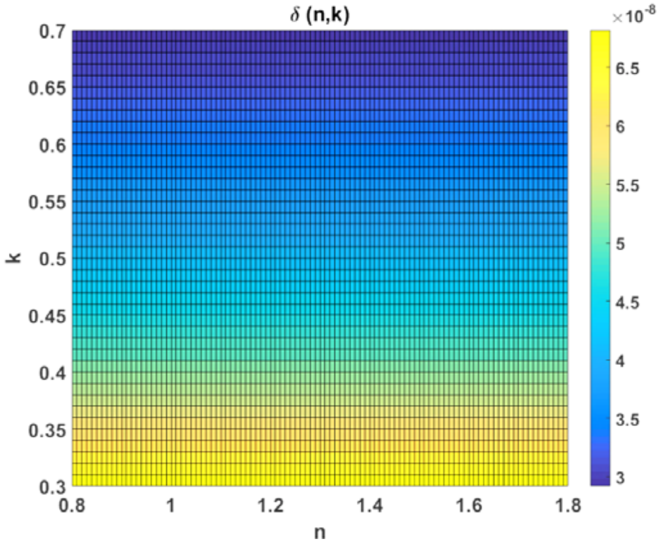

$\boldsymbol{\varepsilon_r} \approx (n - ik)^2 \in$ **[0.73 3.73]**

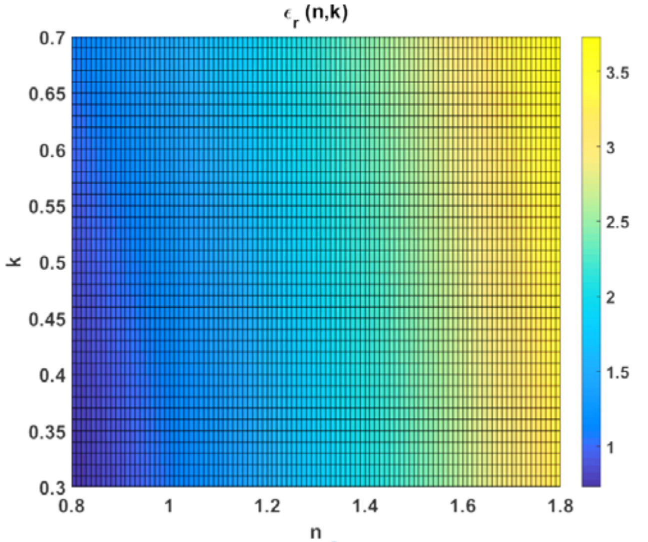

Cross-Ref: for CsI, $\varepsilon_r \leq 9$ @ [113 310] nm

* D. Sertore, INFN Milano – LASA → **detailed n-k measurements needed!**

Scattering effects in Cs_2Te

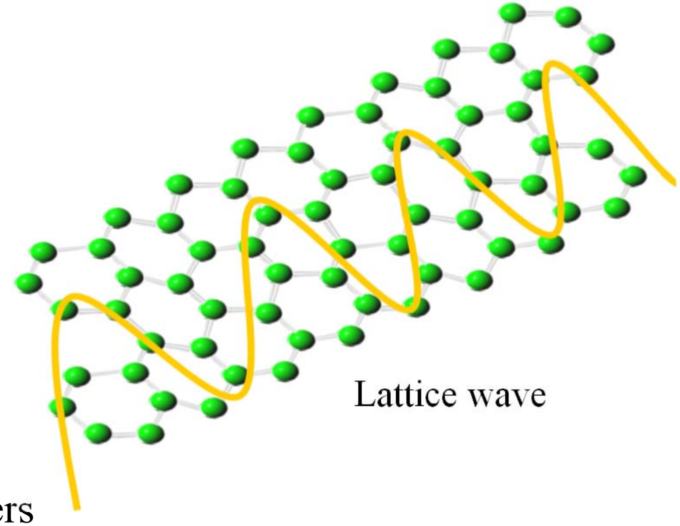

Lattice wave

- ❑ Electron-electron scattering → **dominating for metal cathodes**
- ❑ **Electron-phonon scattering → dominating for semiconductor cathodes**
  - **Polar optical phonon** (vibration within a cell, v_g=0, standing…)
  - **Acoustic phonon (**vibration of a cell, v_g>0, travelling…**)**
- ❑ Electron-impurity(defect) scattering → presumably much weaker effect than others

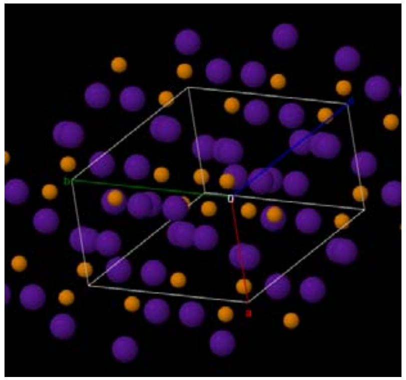

Sketch of a 3D Cs_2Te lattice structure

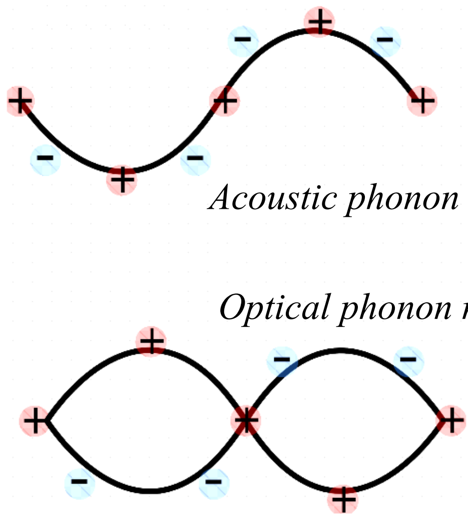

Acoustic phonon mode

Optical phonon mode

Mathematical description of electron-phonon scattering in Cs_2Te

Acoustic phonon $$\frac{1}{\tau_{ac}} = \frac{4m\Xi^2 k(k_B T)}{\pi\hbar^3 \rho v_s^2}\left(\frac{T}{\Theta}\right)^5 W_-\left(5, \frac{\Theta}{T}\right) \propto E_k, E_g, T$$

Polar optical phonon $$\frac{1}{\tau_{pop}} = 2\omega_q\left[2\frac{1}{\exp\left(\frac{\hbar\omega_q}{k_B T}\right) - 1} + 1\right]\frac{16u^2 + 18u + 3}{3(1+2u)\sqrt{u(u+1)}} \propto E_k, E_g, T$$

Matthiessen's rule $$\frac{1}{\mu} = \sum_i \frac{1}{\mu_j} \quad \rightarrow \quad \frac{1}{\tau} = \sum_i \frac{1}{\tau_j}$$

$hk = 2\pi\sqrt{2mE_k}$ $\qquad E_k = h\omega - E_g - E_a$ $\qquad u = E_k/E_g$

→ **Cs2Te specified band structural properties not available**

→ **In order to calculate scattering rates, these properties need to be calculated in advance**

Results and Comparisons to Cs3Sb

Physical Property	Calculation for Cs_2Te	Reference to Cs_3Sb
Mass density	$\rho = \frac{4(2M_{Cs} + 1M_{Te})}{\Delta V} \approx \mathbf{3.99\ g/cm^3}$ *	$4.519\ \mathrm{g/cm^3}$
Sound velocity	$v_s = \sqrt{\frac{c_{11}}{\rho}} \approx \mathbf{5484\, m/s}$ **	$5153\ \mathrm{m/s}$
Phonon energy (lowest mode)	$\hbar\omega_q = \frac{4\pi\hbar v_s}{\lambda_{pm}} \approx \mathbf{0.0767 eV}$	0.05 eV
Average ionic radii	$l \approx \mathbf{0.194\ nm}$ ***	0.14 nm
Deformation potential	$\Xi = Dl \approx \mathbf{9.7\ eV}$ ****	7 eV
Bloch–Grüneisen function	$W_{-}\left(5, \frac{\Theta}{T}\right) \approx (\frac{\Theta}{T})^4/4$	
Fine structure coefficient	$\alpha_{fs} = e^2/4\pi\epsilon_0\hbar c \approx 1/137.1$	
Effective mass	$m = \frac{E_g}{E_{Ry}} m_0 \approx \mathbf{0.24\ m_0}$	$0.1176\ m_0$

* Thermal expansion not considered

** Generic elastic constant, $c_{11} = 12\times10^{10}\ N/m^2$

*** Average of the ionic radii of *Cs* and *Te*

**** Mean deformation potential constant $D = 5\times10^8\ eV/cm$

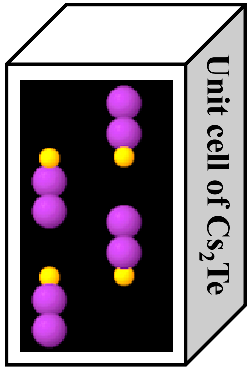

→ **Scattering rates of Cs2Te now can be calculated**

Calculated effective relaxation time

Acoustic phonon scattering, τ_{ac}

Spectrum

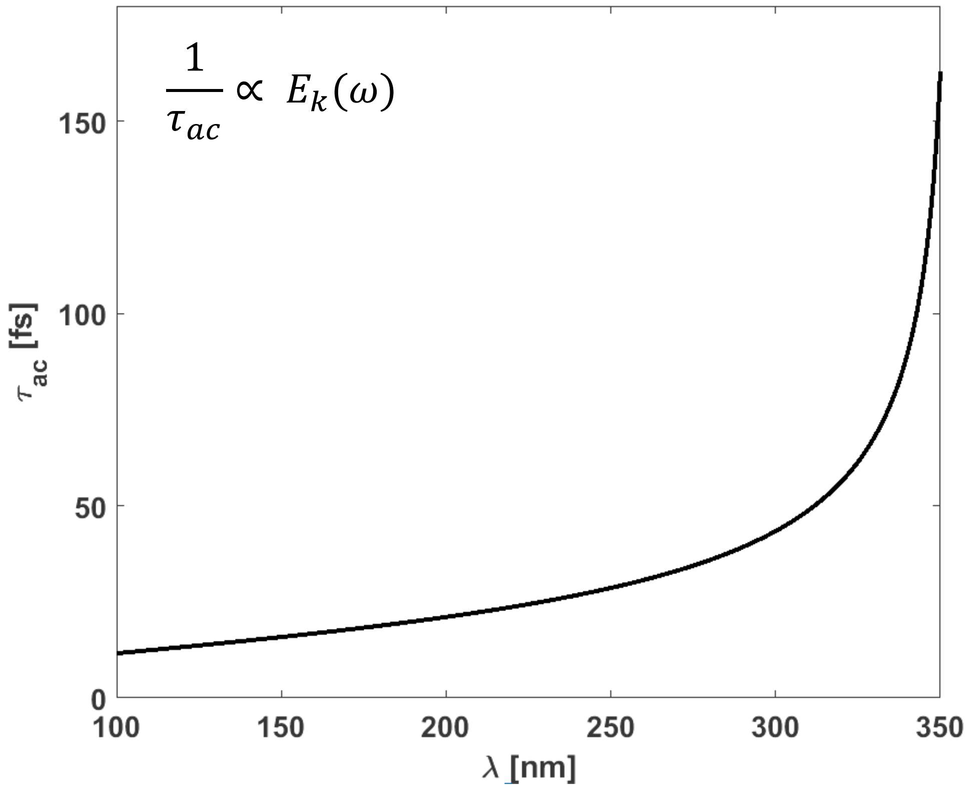

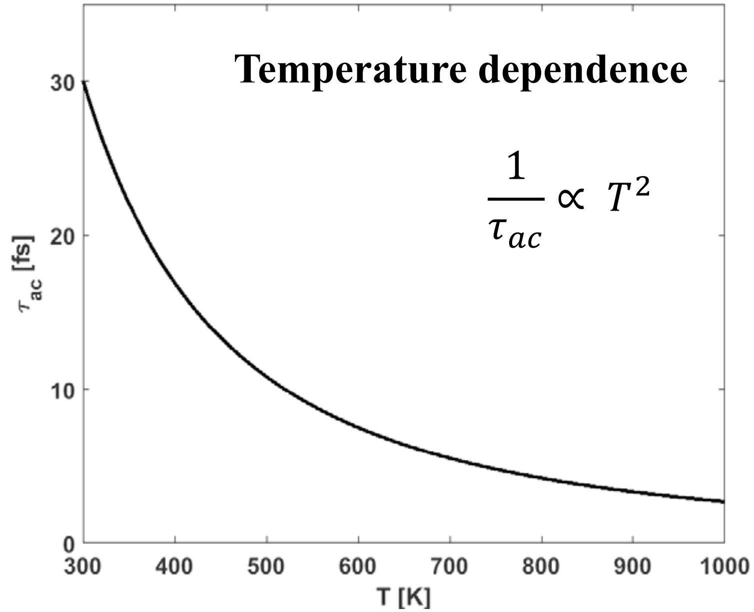

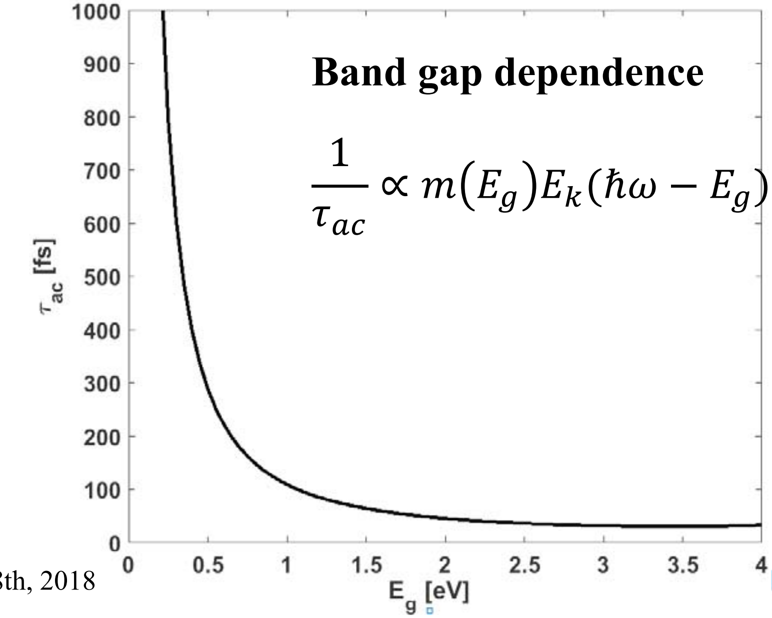

Calculated effective relaxation time

Optical phonon scattering, τ_{pop}

Spectrum

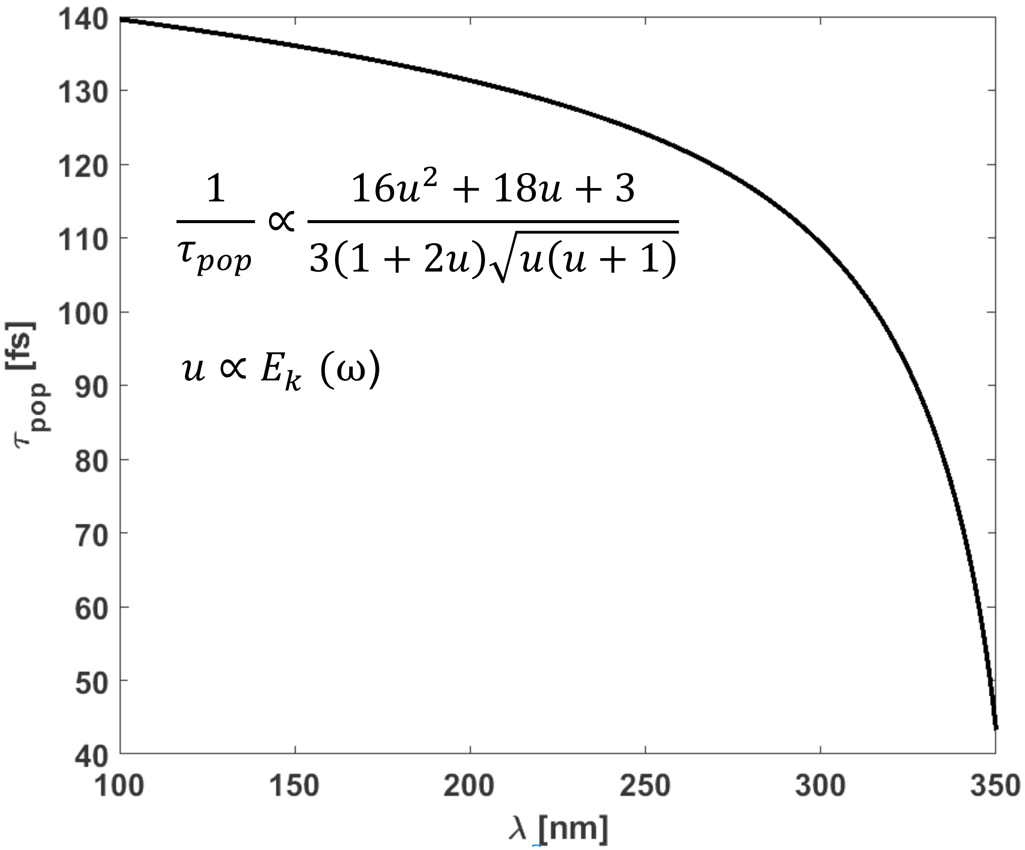

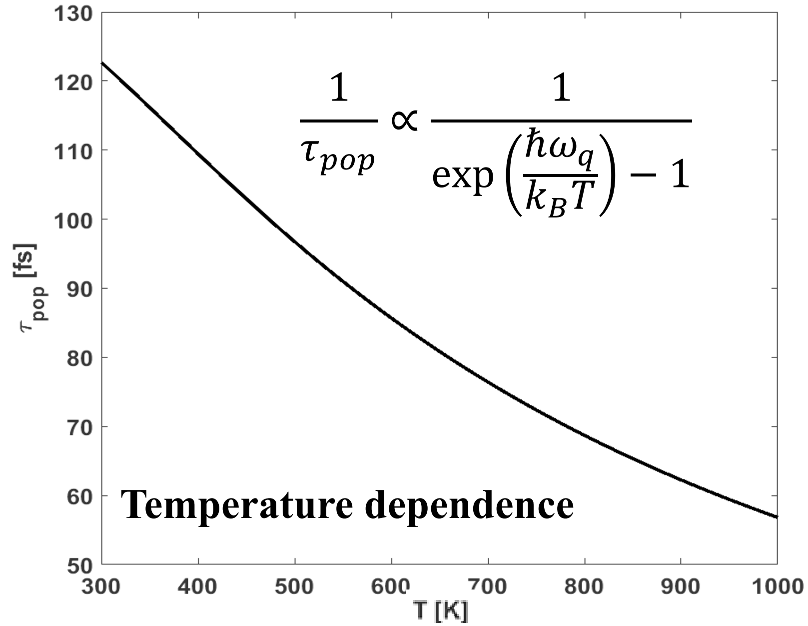

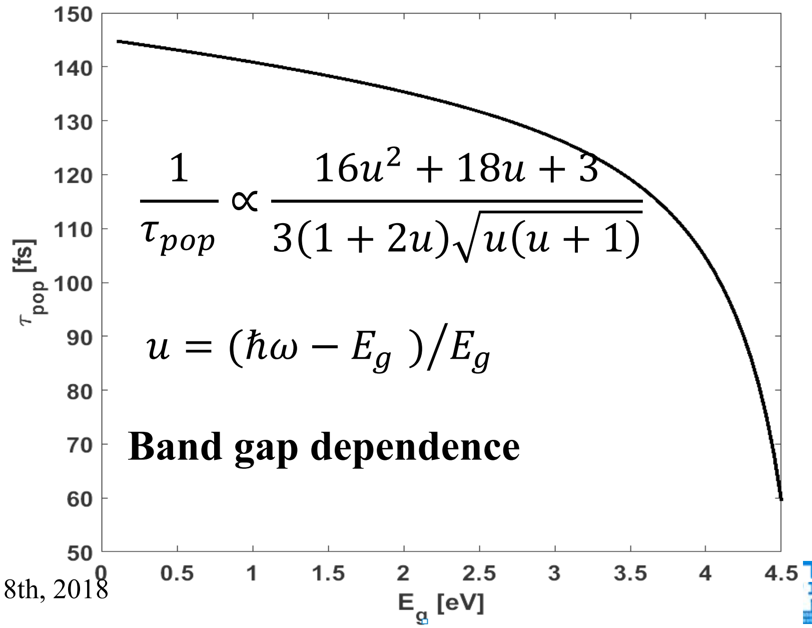

Improving QE formulation

- **Light absorption:** $\boldsymbol{F_{la} \propto 1 - R(\omega, n, k)}$ **IF n-k constant**
- **Electron transport:**
  - ✓ Function of surviving electrons $$f_\lambda(cos\theta) = \frac{\int_0^\infty exp\left(-\frac{z}{\delta} - \frac{z}{l_e cos\theta}\right) dz}{\int_0^\infty \exp\left(-\frac{z}{\delta}\right) dz} = \frac{cos\theta}{cos\theta + p}$$
  - ✓ Ratio of penetration depth to distance between events $p = \frac{\delta}{l_e}$
  - ✓ Effective mean free path when fields penetrating $l_e(E_k) = \tau(E_k)v_d$ $\quad v_d = \mu E_{in}$ $\quad \mu = \frac{q}{m_{eff}(E_g)}\tau(E_k)$

    l_e : **eff. mean free path** $\quad v_d$: drift velocity $\quad E_{in}$: penetrating **full fields** $\quad \mu$: electron **mobility**
  - ✓ Overall integration over escape angle and energy states $$\boldsymbol{F_{et} \propto \int_{\sqrt{E_a/E_k}}^{1} \frac{\Omega^2 d\Omega}{\Omega + m_e\delta(\hbar\omega)/[e\tau_e{}^2\,(r,t)E_{in}(r,t)]}}$$

    Ω: escape angle cosine

Improving QE formulation

- **Electron escape:** $$F_{ee} \propto \frac{4\sqrt{E_k(E_k - E_a)}}{\left[(E_k - E_a)^{0.5} + E_k^{0.5}\right]^2}$$
- **Overall QE:** $$\mathrm{QE} = \{1 - R(\omega, n, k)\} \times \int_{E_a}^{\hbar\omega - E_g} \left\{ \int_{\sqrt{E_a/E_k}}^{1} \frac{\Omega^2 d\Omega}{\Omega + m_e \delta(\hbar\omega)/[e\tau_e^2\,(r,t) E_{in}(r,t)]} \right\} \left\{ \frac{4\sqrt{E_k(E_k - E_a)}}{\left[(E_k - E_a)^{0.5} + E_k^{0.5}\right]^2} \right\} \frac{E_k dE_k}{2(\hbar\omega - E_g)^2}$$

$l_e \propto \frac{e\tau_e^2}{m_e} E_{in}(r,t)$ **effective mean free path**

τ_e	effective relax. time	R	refl. coefficient
m_e	effective mass	δ	penetration depth
E_{in}	penetrating fields		
Ω	escape angle cosine	$\hbar\omega$	photon energy
E_g	band gap		
E_a	electron affinity	E_k	electron energy

→ to be implemented in particle simulations

In addition to overall QE

(n, k) dependencies based on the Drude-Lorentz model

n: refraction index; k: extinction coefficient; $\hat{n} = n + ik$ → optical properties

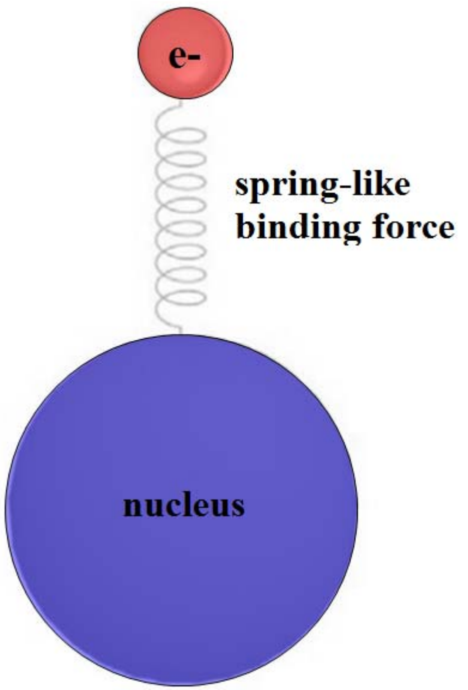

Lorentz oscillator model

- ❑ Dispersive response of materials to external driving force (fields) by influencing the intrinsic wave impedance
- ❑ Intrinsic wave impedance $\eta(\omega) = \frac{\eta_0}{\boldsymbol{n}(\boldsymbol{\omega})}$ $\boldsymbol{n}(\boldsymbol{\omega}) = \frac{c}{v_p}$
- ❑ Lorentz oscillator system
  - "**Dipole** motion" harmonically responding to the driving **field**
  - **Restoring** (Coulomb) force trying to maintain system equilibrium
  - Dampening term modeled by $\boldsymbol{m}_{eff}$/ □

In addition to overall QE

(n, k) dependencies based on the Drude-Lorentz model

n: refraction index; k: extinction coefficient; $\hat{n} = n + ik$ → optical properties

Contributions of free carriers(□)

$$\begin{cases} n^2 - k^2 \propto \omega, \tau(\omega, T, E_k, E_g), E_g \approx A_{static}\Psi + A_{hf}(1-\Psi) + DL_{sum} \\ 2nk \propto \omega, \tau(\omega, T, E_k, E_g), E_g \approx (A_{static} - A_{hf})\Phi - DL_{prod} \end{cases}$$

Contributions of lattice vibration (ω_T)

with

$$\Psi = \frac{{\omega_T}^2({\omega_T}^2 - \omega^2)}{(\omega^2 - {\omega_T}^2)^2 + (\Upsilon\omega\omega_T)^2}, \quad \Phi = \frac{\Upsilon\omega{\omega_T}^3}{(\omega^2 - {\omega_T}^2)^2 + (\Upsilon\omega\omega_T)^2} \quad DL_{sum} = -\frac{(\omega_p\tau)^2}{1 + (\omega\tau)^2},$$

$$DL_{prod} = \frac{\tau{\omega_p}^2}{\omega[1 + (\omega\tau)^2]} \quad \omega_p = \sqrt{\frac{4\pi\rho\alpha_{fs}\hbar c}{m}} \quad m = \frac{E_g}{E_{Ry}} m_0$$

ω: light frequency
c: speed of light
$\hbar$: Planck constant, $h/2\pi$
E_g: band gap energy
E_{Ry}: Rydberg energy, ~13 eV

m_0: electron rest mass
m: electron effective mass
ρ: number density
τ: relaxation time
ω_T: transverse optical mode frequency

ω_p: plasma frequency
α_{fs}: fine structure constant
Υ: Lorentz coefficient
A_{static}: static (dielectric) constant
A_{hf}: high frequency (dielectric) constant

Contributions of free carriers cannot be neglected at RF frequencies?

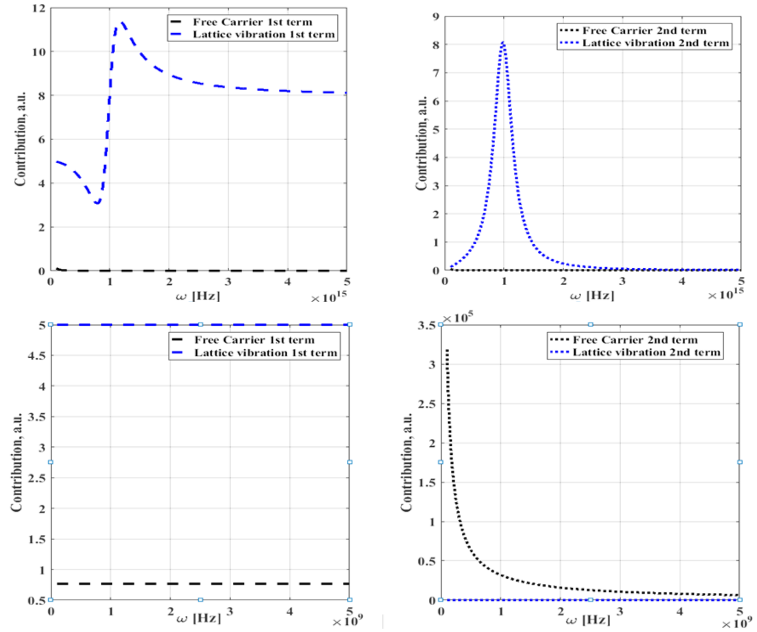

On gun operation (F. Stephan)

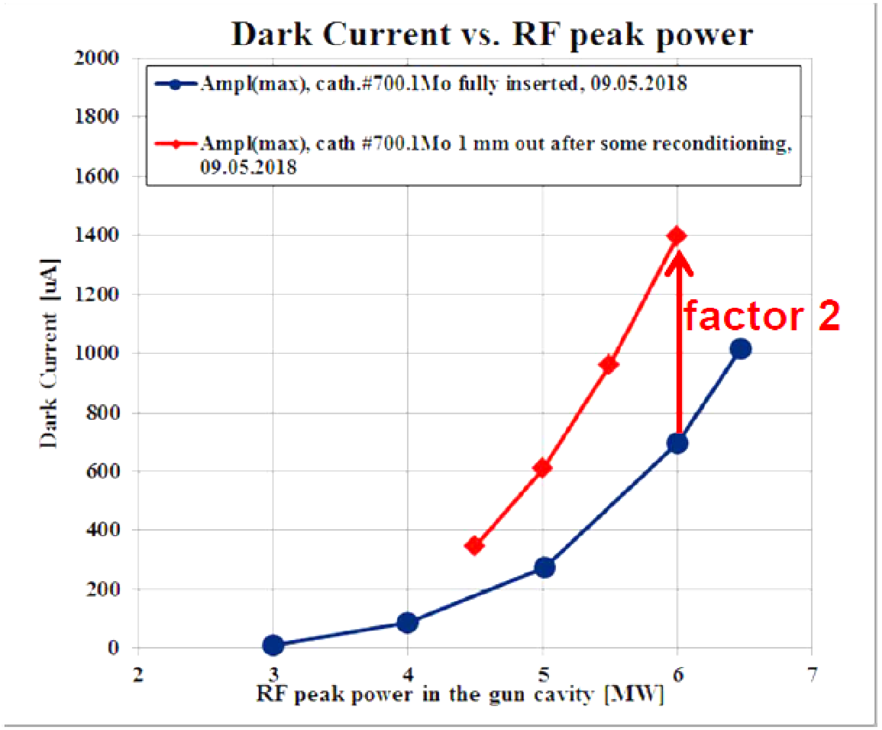

Main conclusion: High dark current is coming from back wall of the gun.

Dark current investigations:

Cathode plug insertion orientation change:

DC images at Low.SCR1. Imain = 380A

Left: normal cathode orientation; Right: rotated by 180deg → similar DC

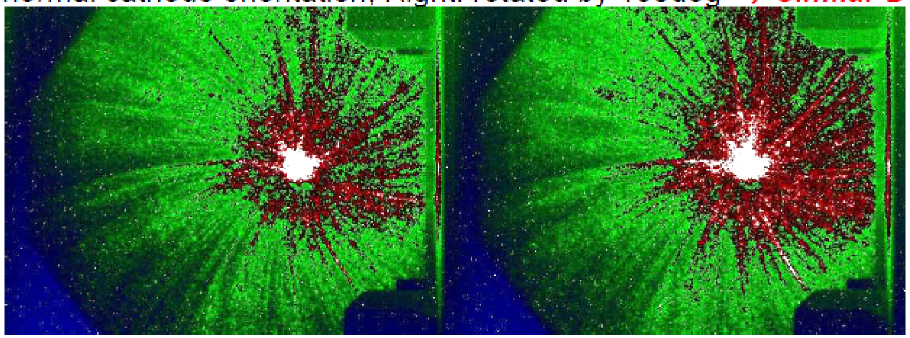

Cathode plug Z position of insertion change:

DC images at Low.SCR1. Imain = 390A

Left: normal cathode positon; Right: cathode plug is out by **1mm** → 2 x DC

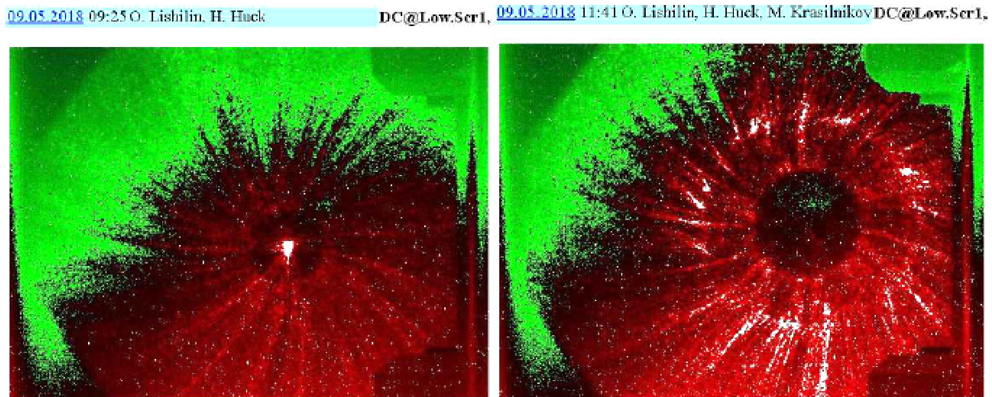

On gun operation

Dark current scan, 6.5 MW, 200 us, cath #700.1

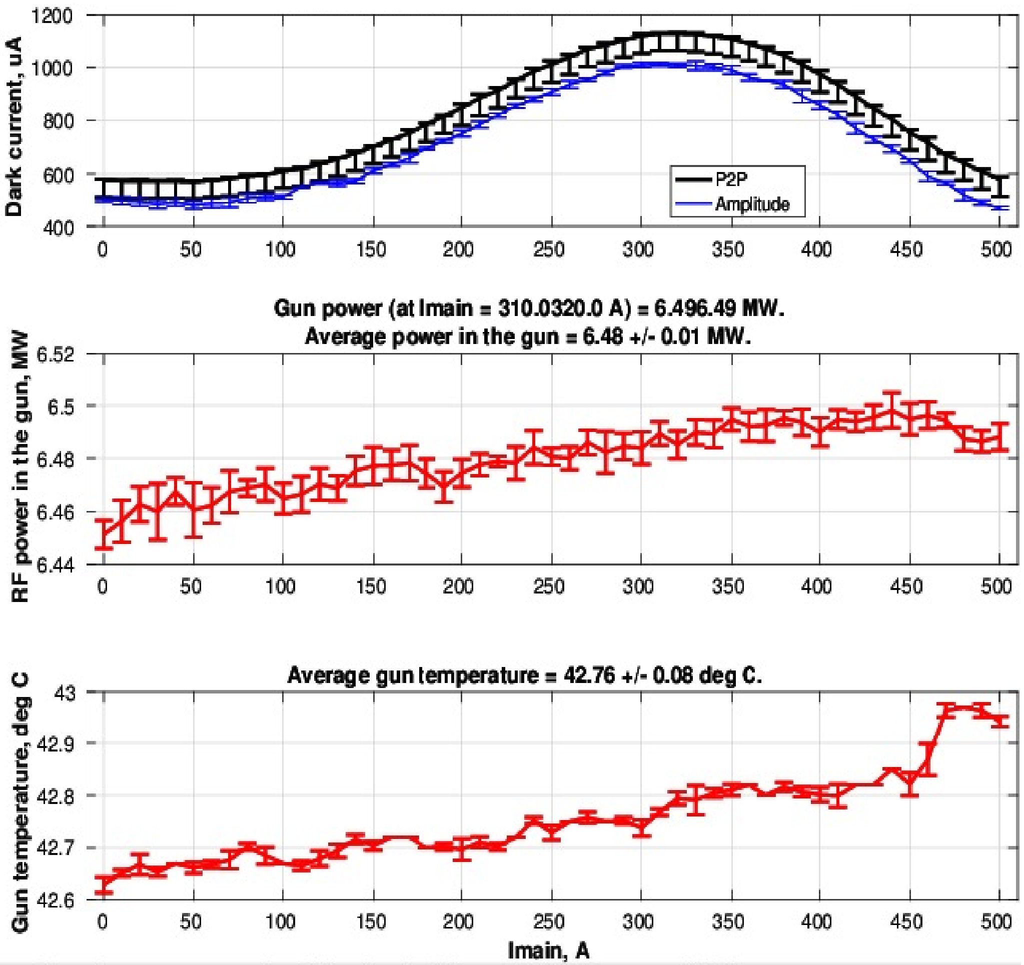

Dark current scan, 6.5 MW, 200 us, cath #700.1 1 mm out

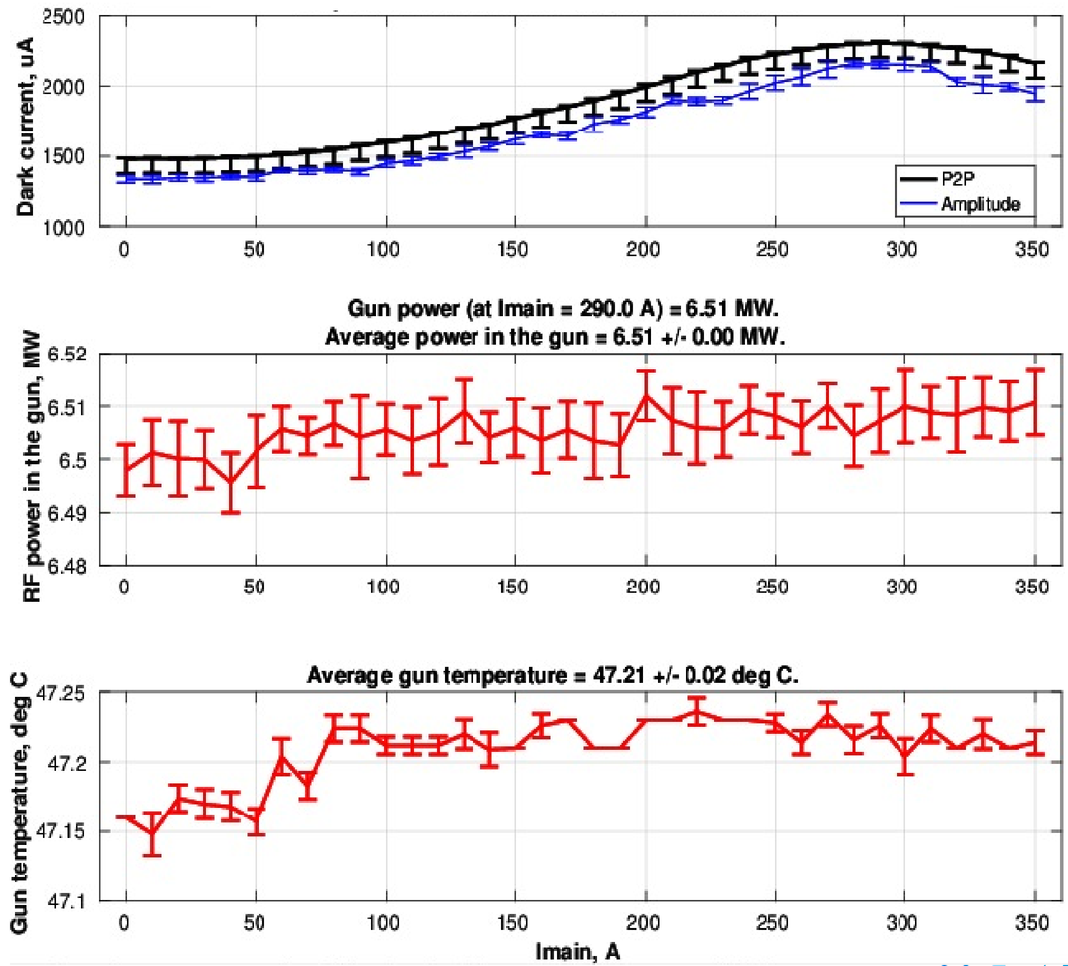

Cathode retraction simulation (M. Krasilnikov)

old results

With -1 mm

- Copper side, about 10% higher
- Cathode center, about 10% lower

2D E-field map |E|(x=0,y,z) of the pi-mode for the nominal position (cath.position 0 mm)

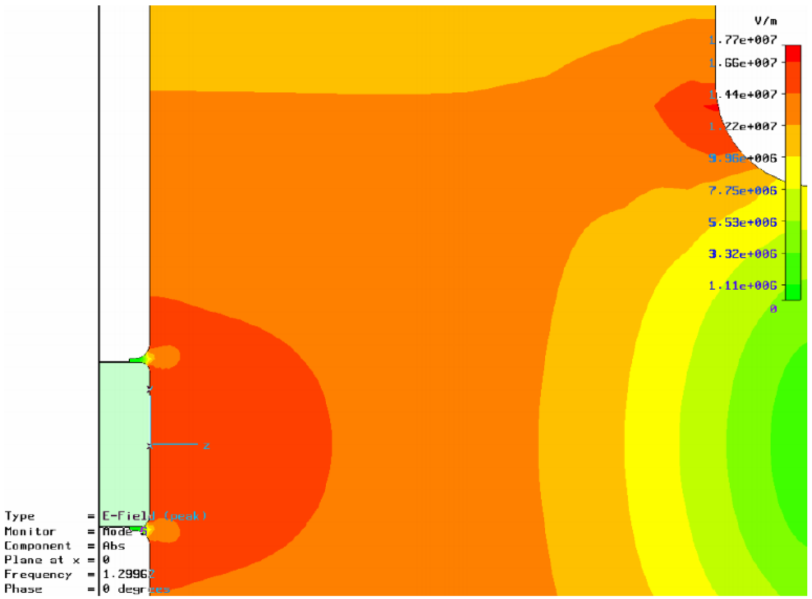

2D E-field map |E|(x=0,y,z) of the pi-mode for the cathode position –1 mm

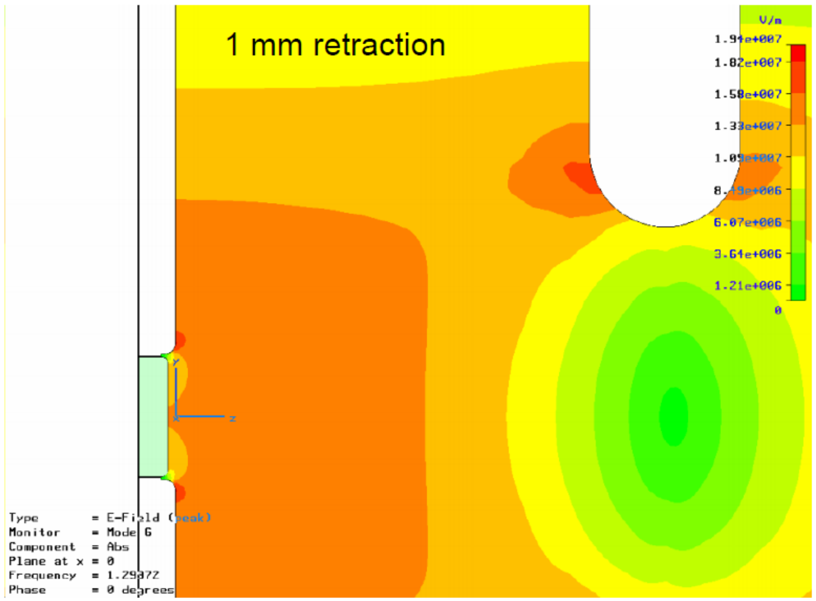

Cathode retraction simulation

old results

Field balance: +1, <+5%; -1, -10%

- Freq detuning: +1, -150 kHz; -1, +100 kHz

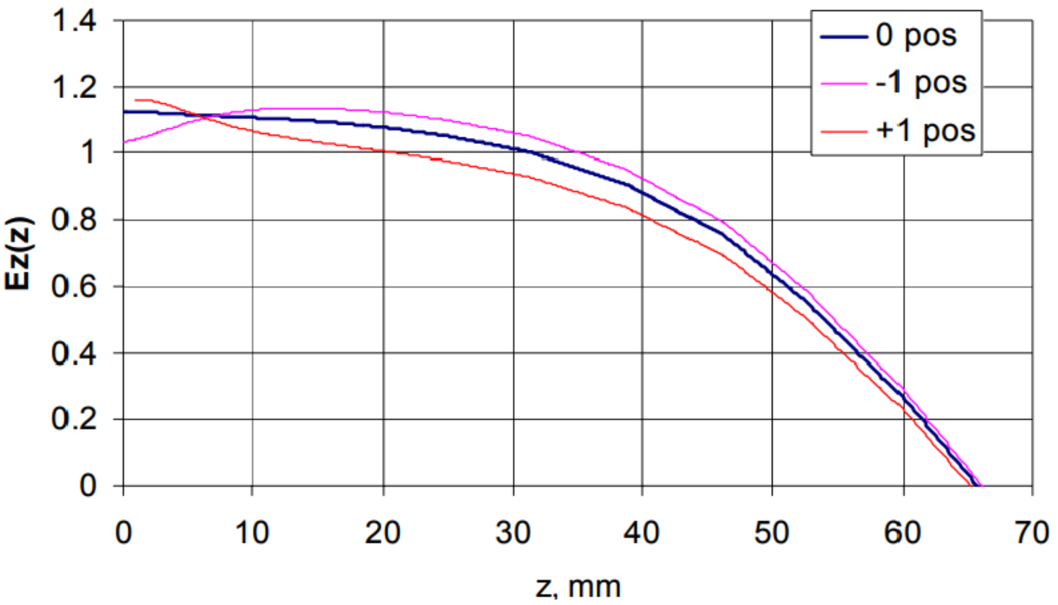

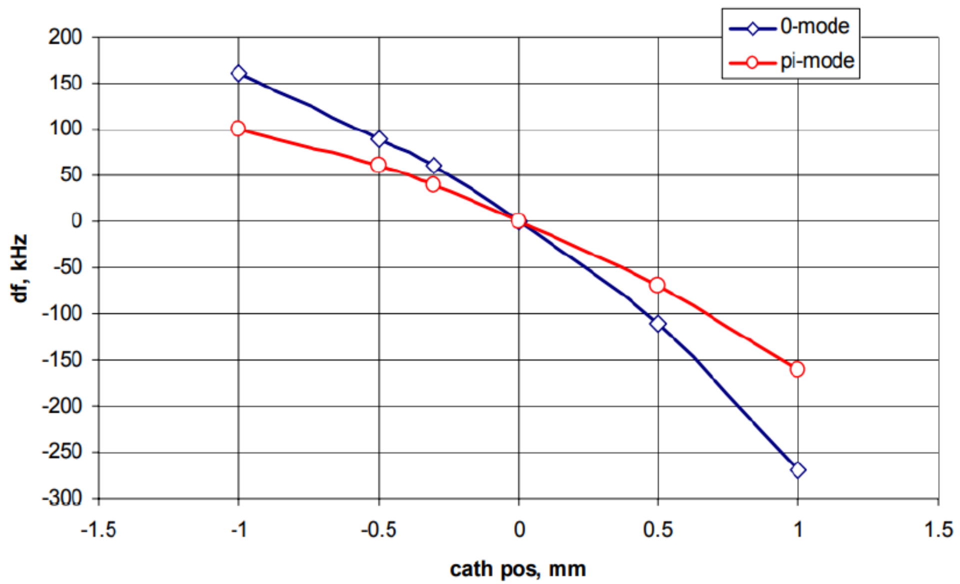

Summary

1. The **traveling wave effect** by the end of coaxial line **affecting beam focusing** (present even for symmetrical coupler case)
2. Main solenoid current for best focusing at 3 screen stations in the low energy section affected by the traveling wave effect, **ΔImain ~ 3A**, partially explaining the experimental results
3. **Time dependent RF kick causing emittance growth →** to be further simulated with space charge
4. RF kick can be compensated by RF focusing for **laser BBA** procedures; Depending on experimental resolution a **kick slope** may still be introduced
5. New **emission modeling** approach proposed

4. Dark current issues at PITZ

Thank you very much for your attention!